EUR 5013 e

COMMISSION OF THE EUROPEAN COMMUNITIES

SOME PHASE EQUILIBRIA AND THERMODYNAMIC CONSIDERATIONS FOR IRRADIATED OXIDE NUCLEAR FUELS

by

P.E. POTTER

1973

Joint Nuclear Research Centre
Karlsruhe Establishment-Germany
European Institute for Transuranium Elements

Paper presented at the

I.A.E.A. Panel Meeting on the Behavior and Chemical State of
Fission Products in Irradiated Fuels
Wien, 6th-11th August, 1972

LEGAL NOTICE

This report is on sale at the addresses listed on cover page 4

at the price of B.Fr. 70.–

Commission of the European Communities
D.G. XIII - C.I.D.
29, rue Aldringen
L u x e m b o u r g
June 1973

EUR 5013 e

SOME PHASE EQUILIBRIA AND THERMODYNAMIC CONSIDERATIONS FOR IRRADIATED OXIDE NUCLEAR FUELS by P.E. POTTER

Commission of the European Communities
Joint Nuclear Research Centre — Karlsruhe Establishment (Germany)
European Institute for Transuranium Elements
Luxembourg, June 1973 — 60 Pages — 36 Figures — B.Fr. 70.—

This paper considers the recent published data on the phase equilibria and thermodynamics of the appropriate oxide systems.

Firstly the binary systems, uranium-oxygen and plutonium-oxygen and the ternary system uranium-plutonium-oxygen and secondly the systems of the major fission products with uranium-oxygen and plutonium-oxygen are considered.

EUR 5013 e

SOME PHASE EQUILIBRIA AND THERMODYNAMIC CONSIDERATIONS FOR IRRADIATED OXIDE NUCLEAR FUELS by P.E. POTTER

Commission of the European Communities
Joint Nuclear Research Centre — Karlsruhe Establishment (Germany)
European Institute for Transuranium Elements
Luxembourg, June 1973 — 60 Pages — 36 Figures — B.Fr. 70.—

This paper considers the recent published data on the phase equilibria and thermodynamics of the appropriate oxide systems.

Firstly the binary systems, uranium-oxygen and plutonium-oxygen and the ternary system uranium-plutonium-oxygen and secondly the systems of the major fission products with uranium-oxygen and plutonium-oxygen are considered.

EUR 5013 e

COMMISSION OF THE EUROPEAN COMMUNITIES

SOME PHASE EQUILIBRIA AND THERMODYNAMIC CONSIDERATIONS FOR IRRADIATED OXIDE NUCLEAR FUELS

Part 1: The Phase Equilibria and Thermodynamics of the Uranium-Plutonium-Oxygen Systems

Part 2: Fission Product Phase Diagrams

by

P.E. POTTER

1973

Joint Nuclear Research Centre
Karlsruhe Establishment-Germany
European Institute for Transuranium Elements

ABSTRACT

This paper considers the recent published data on the phase equilibria and thermodynamics of the appropriate oxide systems.

Firstly the binary systems, uranium-oxygen and plutonium-oxygen and the ternary system uranium-plutonium-oxygen and secondly the systems of the major fission products with uranium-oxygen and plutonium-oxygen are considered.

KEYWORDS

URANIUM OXIDES
URANIUM DIOXIDE
PLUTONIUM OXIDES
PHASE DIAGRAMS
URANIUM
PLUTONIUM
OXYGEN
EQUILIBRIUM
THERMODYNAMICS
FISSION PRODUCTS

PART 1

The Phase Equilibria and Thermodynamics of the Uranium-Plutonium-Oxygen Systems

1. The phase equilibria and thermodynamics of the uranium-plutonium-oxygen systems

The systems U-O, Pu-O, and U-Pu-O are firstly discussed.

1.1. The uranium-oxygen system

Several papers reporting measurements of oxygen potentials of hypostoichiometric UO_{2-x} have appeared recently.

These studies cover the temperature ranges 1873-2173°K (1) using a transpiration technique with H_2O/H_2 mixtures, 1800-2000°K (2) using a technique with control of the oxygen potential by means of the reaction $2\ C + O_2 \rightleftharpoons 2CO$, 2200 - 2400°K (3) using a static system with controlled H_2O/H_2 ratios, and finally in the range 2080 - 2705°K (4) using a transpiration technique with H_2O/H_2 mixtures.

All the data for the oxygen potentials as a function of composition and temperature are shown in Fig. 1.

Tetenbaum and Hunt (5) extended their measurements of oxygen potential in the hypostoichiometric UO_{2-x} region to include measurements of the total pressure of U bearing species in the same temperature range as their previous oxygen potential measurements. These pressures as a function of composition are shown in Fig. 2, and the isotherms show a minimum in the total pressure in agreement with the mass spectrometric data; the position of the minimum is 0,01 - 0,02 atomic ratio units higher than the composition calculated by Edwards et al (6). The values of Pattoret et al (7) of O/U = 1.987 at 2250°K, and Ackermann et al (8) of O/U = 1.994 at 2000°K, are in good agreement with the data of Tetenbaum and Hunt.

A knowledge of the gas phase pressures for oxide systems at temperatures above the melting point is of importance in reactor safety analysis, and Reedy and Chasanov (9) have recently measured the total pressure of the uranium bearing species using a transpiration technique with tungsten as the containment material up

to a temperature of 3390 K. The data obtained,

$$\log p \text{ (atm)} = - \frac{27426}{T} + 7.373$$

are in good agreement with the extrapolated data of Tetenbaum and Hunt corrected for the liquid region using a recent value of 17.7 Kcal/mole (10) for the heat of fusion of UO_2, which is in good agreement with an earlier value of 18.2 Kcal.mole^{-1} (11).

A condensed phase diagram for the region, O/U = 1.5 to 2.2, is shown in Fig. 3 (12).

1.2. The plutonium-oxygen phase diagram

A tentative phase diagram was published in 1966 as a result of the I.A.E.A. assessment of the available data (13). This condensed phase diagram is shown in Fig. 4. The main features which have been further considered by Sari, Benedict and Blank (14) are

a) the continuous solid solution between $PuO_{1.61}$ and PuO_{2-x} above 650°C,

b) the stoichiometry of the "$PuO_{1.61}$" phase, and

c) the maximum oxygen content of the PuO_{2-x} phase in the presence of $PuO_{1.5}$.

The phase diagram which was suggested from this work in which the samples of different O/Pu ratios were quenched from different temperatures down to 5°C is shown in Fig. 5. The main features of this diagram are

a) $PuO_{1.61}$ and PuO_2 do not form a continuous solid solution, at least up to ca. 1000°C,

b) the '$PuO_{1.61}$' has a stoichiometry lower limit of O/Pu = 1.625 and an upper limit of O/Pu = 1.69.

The b.c.c. structure of the C-phase (Fig. 4) has been previously discussed (13) and it was concluded that the O/Pu ratio should be 1.625 and not 1.61, and 4 extra oxygen atoms would be statistically distributed on the 16 ordered oxygen vacancies of the

bixbite unit cell of the b.c.c. $PuO_{1.5}$ low temperature - C-type rare earth oxide. Sari et al stated that it was possible to have a statistical distribution on the 16 vacancies of the bixbite cell if one accomodates 2 more O atoms, giving O/Pu = 1.6875, which is in good agreement wrth the experimental value for the upper phase limit of the C'-phase.

The lattice parameters of the C'-phase increase with decreasing oxygen content and were in agreement with the appropriate values extrapolated from 700 - 900°C (13,15); for O/M = 1.50, a = 11,08 Å

Finally, Sari et al replotted the E,M.F. data of Markin and Rand (16) which gave the partial molal free energy of oxygen ($\Delta \bar{G}_{O_2}$) as a function of O/Pu ratio. These curves are shown in Fig.6, and show the possible existence of a plateau indicating a univariant region (2 condensed phases in a 2-component system) - C' + PuO_{2-x_2}. The lattice parameter measurements of Gardner et al (15) also show irregularities at 700° and 900°C for O/Pu ratios of 1.69 to 1.72 - that is in the univariant region. The two-phase region appears to become wider with increase in temperature. The upper limit of the PuO_{2-x_1}-phase in the presence of C was found to be $PuO_{1.995}$, and not $PuO_{1.98}$ as previously given. The lattice parameter of PuO_2 is 5.3952 ± 0.0005 Å.

Some observations by Marcon, Poitreau, and Roullet (17) on the carbothermic reduction of PuO_2 in the region between PuO_2 and $PuO_{1.5}$ have enabled some information on the Pu-O phase diagram to be obtained in the temperature range 1400 - 1800°C. The gas pressures, mainly CO, were measured as a function of the extent of reaction. If a phase diagram of the form shown in Fig. 4 were appropriate then the C + PuO_{2-x} ($x = 0 \rightarrow 0.4$) would be bivariant and the pressure of CO would fall continuously during the reduction, but two sharp breaks were observed in the curve (Fig. 7) which suggests a more complicated diagram of the type considered by Sari et al.

The various phase fields which were assumed to be present during the reduction process at 1400°C were:

1. PuO_{2-x} (f.c.c.) - carbon with $0 \leq x \leq 0.28$ bivariant

2. $PuO_{1.72}$ (f.c.c.) - $PuO_{1.69}$ (b.c.c.) - carbon — monovariant
3. PuO_{2-y}-carbon with $0.31 \leq y \leq 0.42$ — bivariant
4. $PuO_{1.58}$(b.c.c.) - $PuO_{1.5(hex)}$-carbon — monovariant

The limits appear to vary strongly with temperature above 1400°C and the b.c.c. phase (C', Fig. 5 and c.c., Fig. 8) disappears above 1700°C (Fig. 8).

Dean, Boivineau, Chereau and Marcon (18) measured the partial heat of solution of oxygen ($\Delta \bar{H}_{O_2}$) in PuO_{2-x} using a Calvet microcalorimeter at 1100°C. A very sharp change in curvature was observed at O/Pu = 1.70, a very narrow 2-phase region could be assumed to exist. The oxygen pressure measurements of Riley (19) in the region $1.6 < O/Pu < 2.0$ at temperatures $>700°C$ gave no information on the presence of a univariant region.

1.3 U-Pu-O system

The phase equilibria and thermodynamics of the system have been the subject of a previous I.A.E.A. Vienna panel meeting in 1966 (13). It is however considered useful to survey briefly the additional work on these systems which has been undertaken since the Panel Report was written.

The studies can be divided into two sections, namely

1.3.1. Phase diagrams (including melting points)
1.3.2. Thermodynamic measurements (excluding vaporization studies)

Due to the high temperature gradients in the oxide fuels thermodynamic data are required in the temperature range between 600 and 3000 K.

It is essential that the thermodynamic functions of this system are well defined in order that models developed to describe the chemical behaviour of the complete multicomponent system during 'burn-up' are built on a sound basis.

1.3.1. The phase diagrams

In any considerations of the phase relationships of this system these must be consistent with the binary phase diagrams.

There have been two further phase diagram studies on the U-Pu-O system in the hypostoichiometric region of the diagram since the Vienna oxide panel. Sari, Benedict and Blank (20) have studied the system for Pu/U+Pu ratios of 0.05 - 0.97 from stoichiometric to the fully reduced composition, i.e. until the appearance of a metal phase. Dean, Boivineau, Chereau, and Marcon (18) have also studied the hypostoichiometric region of the phase for Pu/U+Pu ratios between 0.40 and 0.76, and have suggested the presence of a M_7O_{12} type phase with a rhombohedral structure between Pu/U+Pu ratios of 0.60 and 0.90.

Additional studies have also been reported (14,21) for the hyperstoichiometric region of the diagram. The results of Sari et al (20) are shown on the room temperature isothermal section (Fig. 9). It can be seen that up to Pu/U+Pu ratios of ca. 0.20, there will be a range of fluorite structure the amount of oxygen vacancies depending on the Pu valency (from 4 to 3). The previous diagram (22) suggested that this single-phase fluorite region existed up to Pu/U+Pu ratios of ca. 0.30 at room temperature, although this difference may simply be the result of different cooling rates. The area of single-phase fluorite structure depends on the temperature; increasing with temperature (22) (see Fig. 10). The results shown in Fig. 9 were obtained with samples slowly cooled to room temperature and annealed at 200°C, and then slowly cooled. The hypostoichiometric mixed oxides were obtained by partial reduction with hydrogen containing known amounts of water. For complete reduction the experiments were carried out in pure hydrogen. For Pu/Pu+U ratios greater than ca. 0.2, there are two f.c.c. cubic phases, one containing 4-valent Pu and the second probably containing fully reduced 3-valent Pu. The work of Koizumi and Nakamura (35) confirmed the room temperature observations of Sari et al (20) that the two-phase area extends to Pu/U+Pu ratios of ca. 0.20.

A region of transition from f.c.c. to b.c.c. exists between 45 and 50 % PuO_2 (the shaded area in Fig. 9). There is a large region of b.c.c. single-phase oxide for the region with Pu/U+Pu ratios between 0.5 and 0.97. The mixed oxides reduced in pure hydrogen at 1800°C contained a metallic phase when allowed to cool in vacuum, under these conditions it would be expected that the U^{4+} would be reduced, as in the binary system. The metallic phase is in equilibrium with a f.c.c. or a b.c.c. phase and probably also with the hexagonal phase as in the Pu-O system. The lattice parameters of all the phases are shown in Fig. 11. The region in which metal and fully reduced oxide are present will be discussed later.

The results reported by Dean at al (18) for the Pu/U+Pu ratios of 0.4 to 0.7, indicate that up to 0.6 for this ratio there are two f.c.c. phases present and above 0.6, the two phases present are a f.c.c. phase and a rhombohedral phase in place of the b.c.c. phase found by Sari et al. The lattice parameters for the hypostoichiometric region of the U-Pu-O system given by Dean et al are shown in Fig. 12. A super-lattice was present with a lattice parameter twice that shown on Fig. 12; the lattice parameter of this rhombohedral phase varied little between 80 and 90 at % Pu, and the angle α remained fairly constant and close to 89.5°. For Pu/U+Pu ratios greater than 0.9 it was assumed that a two-phase region exists containing a b.c.c. and a f.c.c. phase. Fig. 12 again shows a deviation from Vegard's law for the fully reduced oxide in the presence of a carbide phase - the oxide was reduced with carbon. The carbide is probably a dicarbide or sesquicarbide.

Some high temperature studies have been made using both D.T.A. (20) and high temperature X-ray diffraction (18). The limits of the immiscibility gap as a function of temperature and Pu concentration were determined between 400 and 650°C (20), and similar behaviour to that found earlier namely a decrease in critical temperature with decrease of Pu content (Fig. 13)

A section for Pu/U+Pu = 0,97 obtained from the D.T.A. measurements

(20) is given in Fig. 14. However, the high temperature X-ray dilatometry and electrical resistivity data (18) in the temperature range 400 - 700°C, for Pu/Pu+U ≒ 0.76 suggest a rather more complicated section than that at Pu/Pu+U = 0.97. (Fig. 15)

The fact that for two-phase systems the lattice parameters of the more oxidised phase lie close to the Vegard's law line between UO_2 and PuO_2 indicates that the Pu concentrations in both phases are little different.

The region of the U-Pu-O system containing the two-phases U-Pu metal + the fully reduced oxide, a solid solution between UO_2 and $PuO_{1.5}$, is now considered. The equilibria in this two-phase field can be calculated by assuming that both the U-Pu liquid alloy and the oxide solid solution are both ideal solutions.

For the region $U_{1-x_1}Pu_{x_1}$ (liquid) + $U_{1-x_2}Pu_{x_2}O_{2-0.5x_2}$ (solid) the oxygen potential for the two reactions

$$U(\text{dissolved in Pu}) + O_2(\text{gas}) \rightleftharpoons UO_2(\text{dissolved in } PuO_{1.5})$$

and

$$Pu(\text{dissolved in U}) + \tfrac{3}{4}\, O_2(\text{gas}) \rightleftharpoons PuO_{1.5}(\text{dissolved in } UO_2)$$

must be the same.

The oxygen potentials are given by

$$RT\ln p_{O_2} = \Delta\bar{G}_{UO_2 \text{ dissolved}} - \Delta\bar{G}_{U \text{ dissolved}}$$

and

$$RT\ln p_{O_2} = \tfrac{4}{3}\,\Delta\bar{G}_{PuO_{1.5} \text{ dissolved}} - \tfrac{4}{3}\,\Delta\bar{G}_{Pu \text{ dissolved}}$$

where $\Delta\bar{G}_{UO_2 \text{dissolved}}$ etc. are the partial molal free energies of the components, and for ideal solutions,

$$\Delta\bar{G}_{UO_2} = \Delta G^{o}_{f\ UO_2(\text{solid}} + RT\ln(1-x_2)$$

$$\Delta\bar{G}_{PuO_{1.5}} = \Delta G^{o}_{f\ PuO_{1.5}(\text{solid})} + RT\ln x_2$$

$$\Delta \overline{G}_U = RT\ln(1-x_1)$$

$$\Delta \overline{G}_{Pu} = RT\ln x_1,$$

where ΔG_f^o are the standard free energies of formation, and equating the two expressions for $RT\ln p_{O_2}$

$$4\,\Delta G^o_{f\ PuO_{1.5}} - 3\,\Delta G^o_{f\ UO_2} = 3\ RT\ln\left(\frac{1-x_2}{1-x_1}\right) + 4\ RT\ln\frac{x_1}{x_2}.$$

The results of some computer calculations (23) for 1600° and 2000°K are shown in Fig. 16. The metal phase will always be richer in uranium than the oxide solid solution.

The phase structure of the fully reduced UO_2 - $PuO_{1.5}$ solid solution, and the lattice parameters of this phase have been previously discussed by the Vienna panel, there was a great difference in the lattice parameters depending on the method of preparation (Fig. 17). Three methods of preparation gave different lattice parameters for solid solutions whose compositions were stated to lie on the line joining UO_2 and $PuO_{1.5}$. The alloys prepared by reduction in hydrogen were quite close to the values expected for a pseudo-binary section, however, when the reduction was carried out using metal or carbon the lattice parameters were considerably higher than those of the hydrogen reduction. The data of Sari et al (20) in the presence of metal and those of Dean et al (18) in the presence of, probably, sesquicarbide show a similar deviation.

In the presence of metal the oxide solid solution will contain a greater amount of Pu than the nominal composition, and so the lattice parameters will be closer to the Vegard's law line. For the oxides reduced with carbon and described as 'in the presence' of carbon, and if the second phase is sesquicarbide, the sesquicarbide will be richer in uranium than the oxide phase and thus the same interpretation as given for the oxide in the presence of metal would be applicable to explain the high lattice parameters.

The equilibria for the region $U_{1-x_2}Pu_{x_2}O_{2-0.5x_2}$ (solid) + $U_{1-x_3}Pu_{x_3}C_{1.5}$(solid) is given by

$$3\left[\Delta G^{\circ}_{f<UC_{1.5}>} - \Delta G^{\circ}_{f<UO_2>}\right] + 4\left[\Delta G^{\circ}_{f<PuC_{1.5}>} - \Delta G^{\circ}_{f<PuO_{1.5}>}\right] = 4RT\ln\frac{x_3}{x_2} - 3RT\ln\left(\frac{1-x_3}{1-x_2}\right)$$

Some calculated equilibria for this region are shown in Fig. 18 for 1800°K.

Finally, in considering the phase diagram, results for the hyperstoichiometric region reported by Benedict and Sari (3) are shown together with the results for the hypostoichiometric region in Fig. 19.

1.3.1a. The liquidus-solidus of the U-Pu-O system

Because of the redistribution both of oxygen and uranium and plutonium in a fast reactor fuel operating under conditions where the centre temperatures are very close to the melting points of the oxide or indeed sometimes exceed the melting temperature, it is important to have information on the effect of stoichiometry and plutonium-concentrations on the solidus-liquidus temperatures. The liquidus-solidus of the U-Pu-O system reported to the previous Vienna Panel for stoichiometric solid solution (24) are reproduced in Fig. 20. The addition of Pu lowers the liquidus and solidus temperatures.

Some measurements of the effect of stoichiometry on the liquidus-solidus of the system have been reported by Aitken et al (25). The liquidus temperature changes little and the difference in solidus temperature when the O/M ratio changes from 2.00 to 1.92 is ca. 80°C for Pu/U+Pu ratios of 0.2.

1.3.2. The Thermodynamic data for the U-Pu-O system

Using the extrapolated oxygen potential data of Markin and McIver (26), reported in the oxide panel meeting together with

the thermodynamic data for the gas phase molecules UO_3, UO_2, UO, U and PuO_2, PuO, Pu obtained from vapour pressure measurements of the metal or the appropriate binary systems Markin and Rand (27) have calculated the individual species gas pressures and the total pressure above the U-Pu-O system as a function of O/U+Pu for a given Pu/U+Pu ratio. Some results of the calculations are shown in Fig. 25 for 2000°K, and the total pressure passes through a minimum at $\sim MO_{1.967}$; this, however, is not associated with a congruently vaporizing composition, nor with a constant vapour composition.

These calculations and experimental measurements on this system which will be discussed are of great significance to the redistribution of U and Pu via the gas phase in a fuel element.

Experimental measurements on the vaporization of the U-Pu-O system have been reported by Ohse and Olson (28), Battles et al (29) and Dean at al (18). Some earlier work at Fontenay-aux-Roses on the vaporization was reported to the Vienna Panel (13).

The conditions of the various vaporization experiments are shown in Table 1.

TABLE 1

Vaporization experiments on U-Pu oxides

Reference	Composition (initial)	Temperature Range (°K)	Method
28	$U_{0.85}Pu_{0.15}O_{2-x}$ $x = 0$ to 0.06	1800-2350	Knudsen effusion target collection and mass spectrometry
29	$U_{0.8}Pu_{0.2}O_{2-x}$ $x = 0$ to 0.008	1905-2411	Knudsen effusion mass loss, and mass spectrometry
18	$U_{0.5}Pu_{0.5}O_{1-x}$ $U_{0.76}Pu_{0.24}O_{2-x}$	1814-2220	Knudsen effusion and target collection
13	$U_{0.1}Pu_{0.9}O_{2-x}$ $U_{0.2}Pu_{0.8}O_{2-x}$	1800-2500	Knudsen effusion and target collection

Ohse and Olson (28) heated the samples of mixed oxides in tungsten effusion cells using an electron beam furnace. The technique employed allows the determination of partial pressures of the gas phase components by simultaneous application of the effusion collection technique and mass spectrometric analysis. The relative abundances of PuO, PuO_2, UO_3 and UO_2 in the vapour above $U_{0.85}Pu_{0.15}O_{2-x}$ whose x ranged from 0 to 0.06 were determined. These workers took great care in avoiding the inherent problems of fragmentation, particularly that of UO_3 by using electron energies below the fragmentation potentials, and by use of direct calibration and obtained the relationship (e.g. for UO_2)

$$I^+_{UO_2} \cdot T = p_{UO_2} \cdot C_{UO_2}$$

where C is a specific ion sensitivity factor . All the specific ion sensitivity factors for the various gas phase species were determined, and thus all the partial pressures could be determined at any composition by measurement of the ion currents.

Fig. 22 shows the isothermal rate of the composition change of the solid solution $U_{0.85}Pu_{0.15}O_2 \pm x$ as a function of time. A quasi-congruent evaporating composition close to O/M = 1.97 is approached from both sides of the composition range. The partial pressures of PuO_2, PuO, UO_3, and UO_2 over $U_{0.85}Pu_{0.15}O_{1.969}$ in the temperature range from 2000-2350°K are given in Fig. 23. From these relationships the second law partial enthalpy and entropy changes at this quasi-congruently evaporating composition of O/M = 1.969 assuming the change in Cp to be negligible in the measured temperature range were obtained. Because of the rapid change of composition at both extremities of the substoichiometric single phase region (Fig. 21), $\log(I^+,T)$ or $\log_{Pi}$ versus $\frac{1}{T}$ measurements cannot necessarily be interpreted as the partial enthalpy values.

Finally using the modified data for $\Delta G^o_{f(PuO_2)}$

$$\text{namely } \Delta G^o_f = -102{,}700 + 3.16\ T \text{ cal/mole}$$

compared with the previous data

$$\triangle G_f^o = - 113,100 + 4.35\ T \text{ cal/mole}$$

obtained from earlier assessment of Ackermann, Faircloth, and Rand (30), whilst the new value was obtained from the more recent measurements of Ohse and Ciani (31) of the Pu-O system. Together with the pressure data for the gas species, Ohse and Olson obtained very good agreement for the oxygen potential of the system at 2108°K, namely --117 to -118 Kcal.mole O_2^{-1} from both the reactions

$$2(PuO) + (O_2) \rightleftharpoons 2(PuO_2)$$

and

$$2(UO_2) + (O_2) \rightleftharpoons 2(UO_3)$$

The oxygen potential is also in good agreement with the predictions assuming ideal solid solution in the solid.

The investigations of Battles et al (29) are comparable although the Pu concentration was slightly higher - the compositions examined were $U_{0.8}Pu_{0.2}O_{2-x}$ with $1.92 \leqslant O/M \leqslant 2.00$.

The Knudsen effusion cells used in the study were made of W, Re and Ir. Vapour species typical of the vaporization of W or Re oxides were observed when the mixed oxide ($O/M \sim 2.0$) was heated at ca. 1200°C or higher in W or Re effusion cells. Because of this incompatibility of the oxide with W and Re, iridium cells were used.

The ion intensities of UO^+, UO_2^+, UO_3^+, PuO^+ and PuO_2^+ were measured as in the experiments of Ohse and Olson, and these were the only gas phase species detected.

A curious feature of these measurements is that the ion extensity of UO_3^+ was determined using an ionising electron energy of 15 eV, which is greater than the fragmentation potential of UO_3^+, which was given by Pattoret et al (32) as 13.6 ± 1 eV The fact that UO^+ was also found could again have been formed by the fragmentation of UO_2^+, the fragmentation potential being

13.6 ± 0.5 eV. The interpretation of the $\log(I^+T) - \frac{1}{T}$ plots can only be made providing the composition of the solid for a series of measurements does not change markedly with time, that is, one is close to a quasi congruent vaporization, and that this point does not change much with temperature. The values for the heat of sublimation from the two studies are shown in Table 2, which clearly shows the discrepancy in the data for UO_3.

At 2241°K, the vapour pressure was calculated for the system by determining the rate of effusion from the oxide, and from the ion intensities which showed UO_2^+ to be the predominant species, the pressure of the gas was calculated. The total pressure decreased significantly as the O/M ratio decreased from 2.0 to about 1.94. The partial pressure derived from the ion intensivities by assuming that the ionization cross sections and multiplier efficiencies are assumed equal. The estimated partial pressures of the species are shown in Fig. 24. There appears to be no minimum as predicted in the calculations and found by Ohse and Olson in the range of O/M from 1.92 to 2.00. There is a discrepancy in the pressures of oxygen gas calculated from the two equilibria

$$UO_2(g) + O(g) \rightleftharpoons UO_3(g)$$

$$PuO(g) + O(g \rightleftharpoons PuO_2(g)$$

and the pressures are higher than predicted from the extrapolation of Markin and Rands data even for curve A (Fig. 25).

It is appropriate here to mention the earlier work reported by Pascard (13), for U-Pu oxides containing 10, 20, and 25% Pu the data for which were reported only in terms of U and Pu bearing species indicating that the pressures of U bearing species are greater than those of Pu bearing species for O/M ratios between 1.95 and 2.00.

The study of Dean et al (18) extends the composition of Pu up to Pu/U+Pu ratios of 0.50 and 0.76. Free energy of formation data

TABLE 2

Enthalpies of vaporization of the gas-phase species above U-Pu oxides.

Composition of solid	Gas species	Temperature Range (°K)	Enthalpy of vaporization Kcals/mole	
			Ref.29	Ref.28
$U_{0.8}Pu_{0.2}O_{2.00-1.92}$ (Ref. 29)	UO_3	1905-2411 (Ref.29)	158.5±2.0	115.8±4.2
$U_{0.85}Pu_{0.15}O_{1.969}$ (Ref.28)	UO_2	2000-2350 (Ref.28)	146.3±1.7	148.4±2.3
	PuO_2		139.4±1.8	141.9±5.0
	PuO		123.4±1.7	124.5±1.3

for $PuO(g)$ and $PuO_2(g)$ were determined from the evaporation of the binary system Pu-O and from the ternary system with Pu/U+Pu = 0.76. PuO_2 gas was found to be more stable than previously reported by Ohse and Ciani

$$\Delta G^{o}_{f(PuO_2)} = -117.700 + 3.05 \text{ cal.mole}^{-1}$$

and this value of PuO_2 suggests that the values for $\Delta \overline{G}_{O_2}$ should be corrected slightly from those given by the extrapolation of the data of Markin and Rand (27). Some specific heat data (Cp) have been reported in the temperature range between 1600°C and the melting points by Affortit and Marcon (33).

Experiments on the thermal diffusion of oxygen in hyperstoichiometric urania - 15% plutonia solid solutions (34) also suggest that there may be a non-linear dependence of $\Delta \overline{G}_{O_2}$ on temperature when $T > 1200°C$.

Some data on the vaporization of $U_{0.5}Pu_{0.5}O_{2.10}$ at 1814°K (18) are also available; and on the basis of the experimental results suggested that the oxygen potentials should be modified, the presence of UO_3 was found to be less than that calculated, but some difficulty would be encountered in defining the composition of the solid for a given pressure measurement.

Measurements of the partial molal heat of solution ($\Delta \overline{H}_{O_2}$) for the mixed oxides with Pu/U+Pu = 0.10 and 0.15 have also been reported, and are in semi-quantitative agreement with those of Markin and Rand.

References:

1. N.A. JAVED, J.Nucl.Materials 43 (1972) 219
2. V.J. WHEELER, J.Nucl.Materials 39 (1971) 315
3. T.L. MARKIN, V.J. WHEELER, R.J. BONES, J.Inorg.Nucl.Chem. 30 (1968) 807
4. M. TETENBAUM, P.D. HUNT, J.Chem.Phys. 49 (1968) 4739
5. M. TETENBAUM, P.D. HUNT, J.Nucl.Materials 34 (1970) 86
6. R.K. EDWARDS, M.S. CHANDRASEKHARIAH, P.M. DANIELSON, J.High Temp.Science 1 (1969) 98
7. A. PATTORET, J. DROWERT, S. SMOES, Thermodynamics of Nuclear Materials (1967) I.A.E.A. Vienna 1968, p.613
8. R.J. ACKERMANN, E.G. RAUH, M.S. CHANDRASEKHARIAH, U.S.A.E.C. report ANL-7048 (1965)
9. G.T. REEDY, M.G. CHASANOV, J.Nucl.Materials 42 (1972) 341
10. L. LEIBOWITZ, M.G. CHASANOV, L.W. MISHLER, D.F. FISCHER, J.Nucl.Mat. 39 (1971) 115
11. R.A. HEIN, P.N. FLAGELLA, U.S.A.E.C. report GEMP-578 (1968)
12. R.E. LATTA, R.E. FRYXELL, J.Nucl.Mats. 35 (1970) 195
13. The plutonium-oxygen and uranium-plutonium-oxygen systems: A thermochemical assessment, I.A.E.A. Technical Reports Series No. 79, I.A.E.A. Vienna 1967
14. C. SARI, U. BENEDICT, H. BLANK, Thermodynamics of Nuclear Materials 1967, I.A.E.A. Vienna 1968, p. 587
15. E.S.GARDNER, T.L. MARKIN, R.S. STREET, J.Inorg.Nucl.Chem. 27 (1965) 541
16. T.L. MARKIN, M.H. RAND, Thermodynamics 1 Proc.Symp.Vienna 1965, I.A.E.A. Vienna (1966) 145
17. J.P. MARCON, J.POITREAU, G. ROULLET, Plutonium 1970 and other actinides (ed.W.N. Miner) Nuclear Metallurgy 17 pt.II New York 1970, The Metallurgical Society of the American Institute of Mining, Metallurgical and Petroleum Engineers Inc. p. 799
18. G. DEAN, J.C. BOIVINEAU, P.CHEREAU, J.P. MARCON, ibid.p.753
19. B. RILEY, Sci.Ceramics 5 (1970) 83
20. C. SARI, U. BENEDICT, H. BLANK, J.Nucl.Mat.35 (1970) 267
21. U. BENEDICT, C. SARI, Euratom Report EUR 4136e(1970)

22. T.L. MARKIN, R.S. STREET, J.Inorg.Nucl.Chem. 29 (1967) 2265
23. P.E.POTTER, Plutonium 1970 and other actinides, p.859
24. W.L. LYON, W.E. BAILY, J.Nucl.Mat.22 (1967) 332
25. E.A. AITKEN, G.K. EVANS, M.G. ADAMSON, T.E. LUDLOW, U.S.A.E.C. report GEAP-12229 (1971)
26. T.L. MARKIN, E.J. McIVER, Plutonium 1965, Proceedings 3rd International Conference on Plutonium (ed.A.E.Kay, M.B.Waldron), London 1967, Chapman and Hall, p.845
27. M.H. RAND, T.L. MARKIN, Thermodynamics of Nuclear Materials 1967, I.A.E.A. Vienna (1968) p.637
28. R.W. OHSE, W.M. OLSON, Plutonium 1970 and other actinides, p.743
29. J.E. BATTLES, W.A. SHINN, P.E. BLACKBURN, R.K. EDWARDS, ibid. p. 733
30. R.J. ACKERMANN, R.L. FAIRCLOTH, M.H. RAND, J.Phys.Chem. 70 (1969) 3698
31. R.W. OHSE, V. CIANI, Thermodynamics of Nuclear Materials 1967, I.A.E.A. Vienna 1968, p.545
32. A. PATTORET, J. DROWART, S. SMOES, ibid. p.613
33. C. AFFORTIT, J.P. MARCON, Rec.Int.Haut.Temp.Ref. 1 (1970)236
34. M.G. ADAMSON, R.F.A. CARNEY, A.N.S. Transactions 14 (1971) 179
35. N. KOIZUMI, Y.NAKAMURA, Ceram.Nucl.Fuels, Proceedings of the international symposium. Nuclear Div., Amer.Ceram.Soc.Spec. Pub. No.2 (ed.O.L.Kruger, A.I. Kaznoff) 1969 Columbus, Ohio, p. 25.

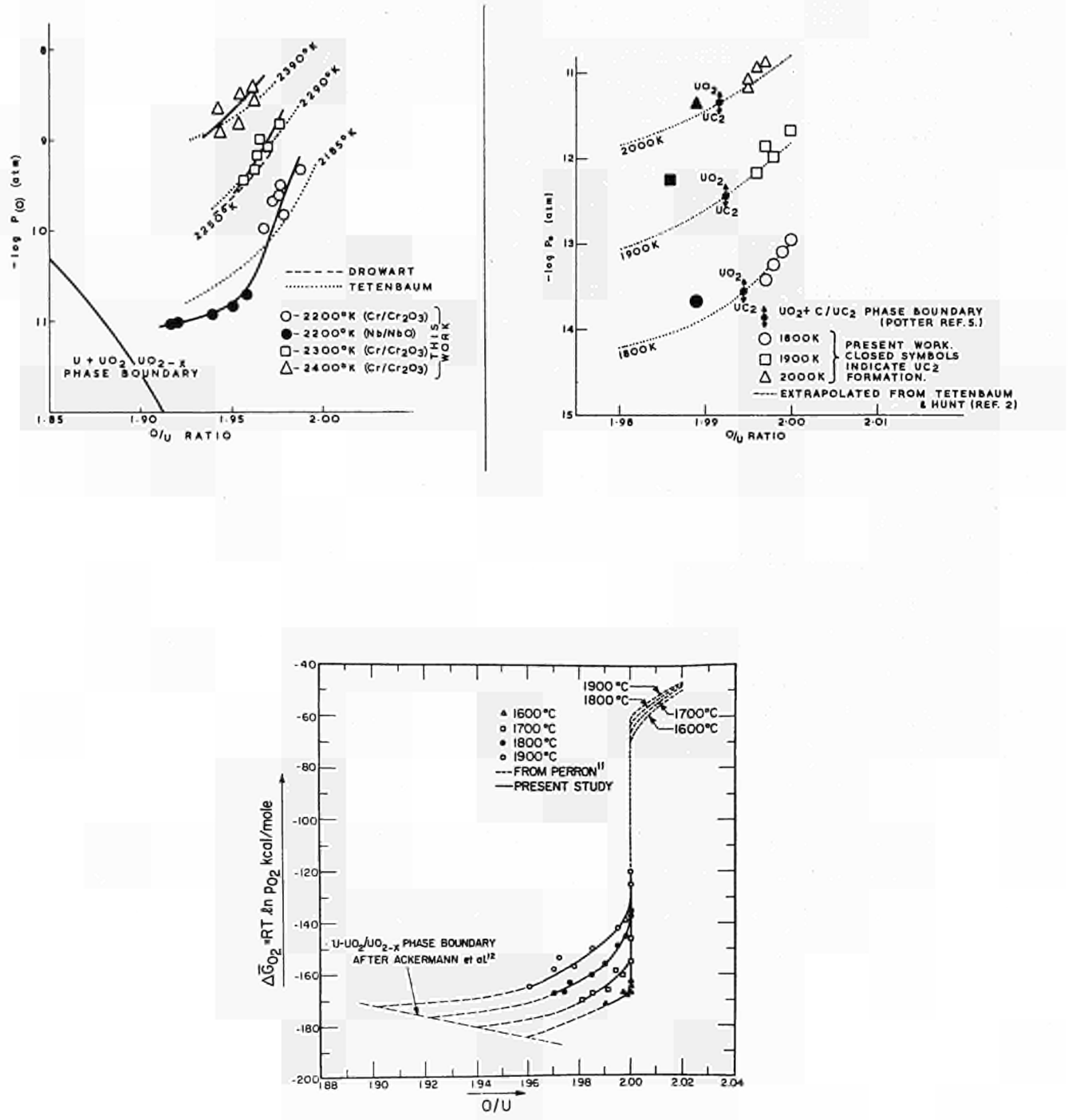

FIG. 1 Oxygen potentials for the uranium-oxygen system

A. Variation of log $P_{(O)}$ with O/U ratio for UO_{2-x} (ref 3)

B. Variation of relative partial molar free energy of oxygen with temperature and O/U ratio for $UO_{2\pm x}$ (ref 1)

C. Variation of equilibrium oxygen pressure (expressed as log P_o) with O/U ratio at various temperatures (ref 2)

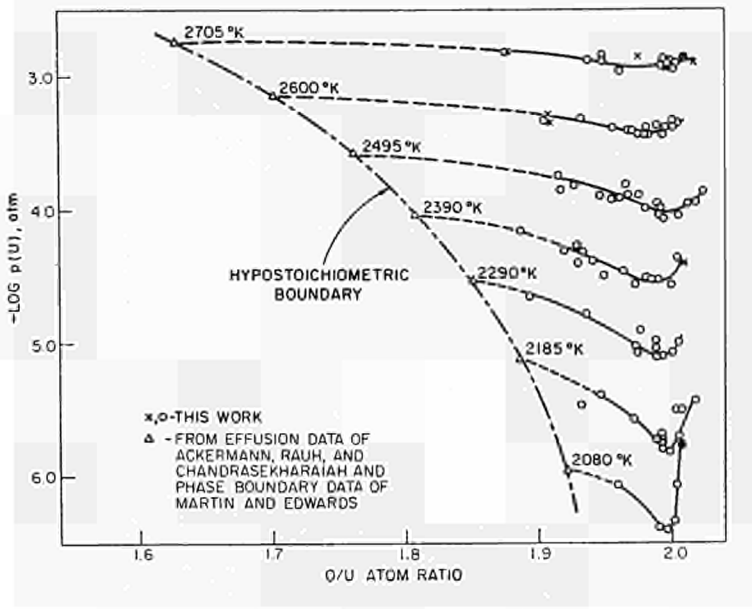

FIG. 2 Total pressure of uranium-bearing species as a function of temperature and urania composition (ref 5)

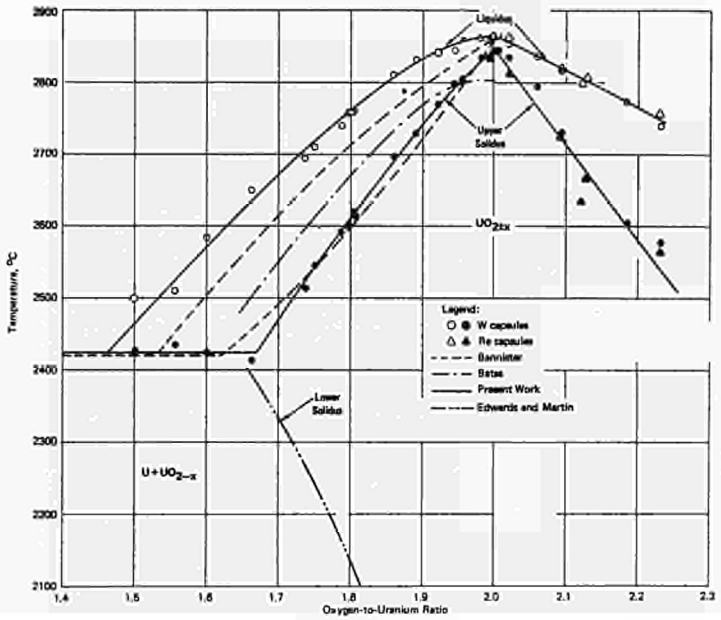

FIG. 3 Partial phase diagram for urania from $UO_{1.46}$ to $UO_{2.23}$ (ref 12)

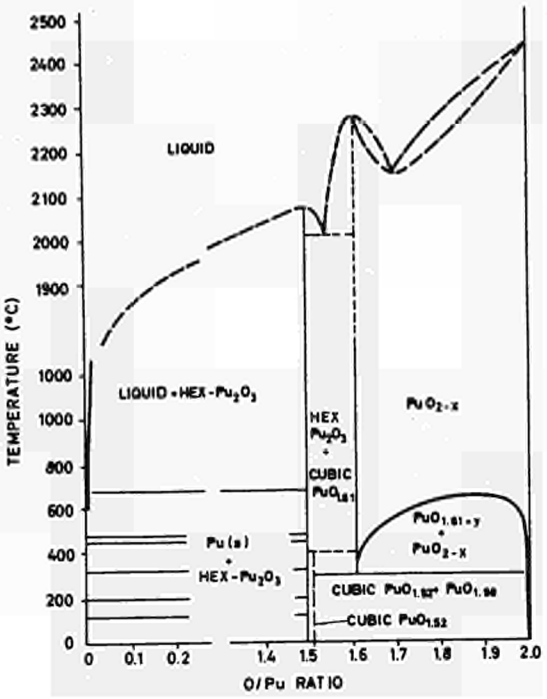

FIG. 4 A tentative plutonium-oxygen phase diagram (ref 13)

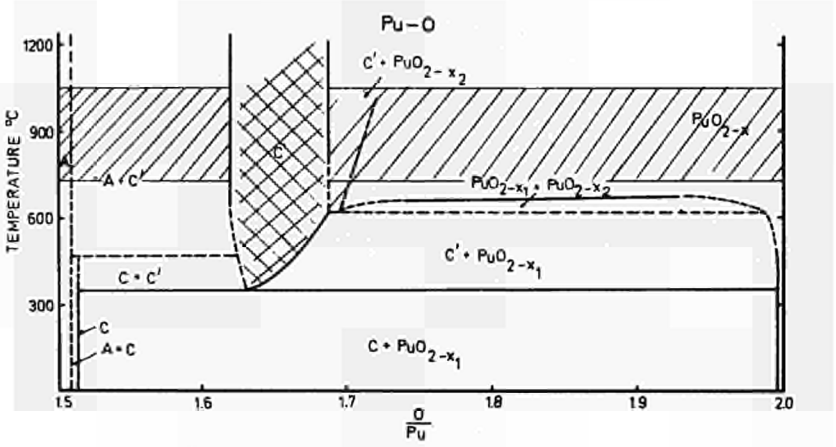

FIG. 5 A plutonium-oxygen phase diagram (ref 14)

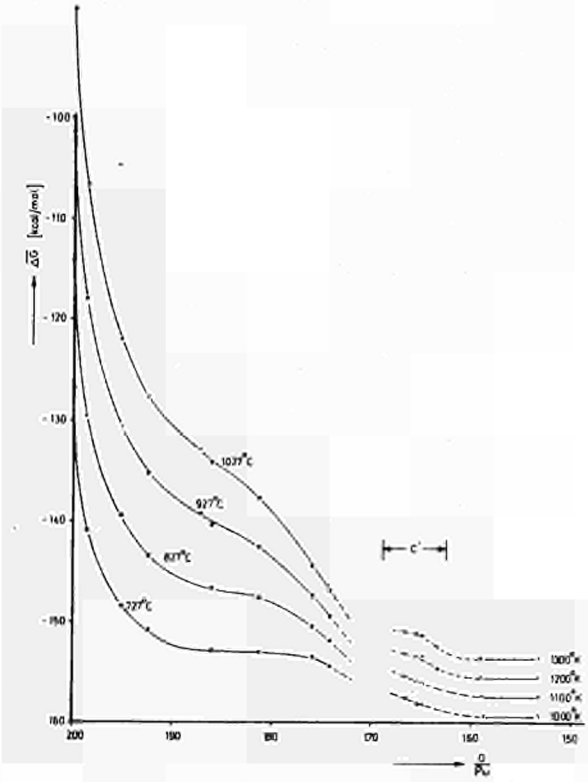

FIG. 6 $\Delta\bar{G}$ (oxygen) versus $^{O}/_{Pu}$ (ref 13)
The region marked by C' gives the α-single phase region (ref 14)

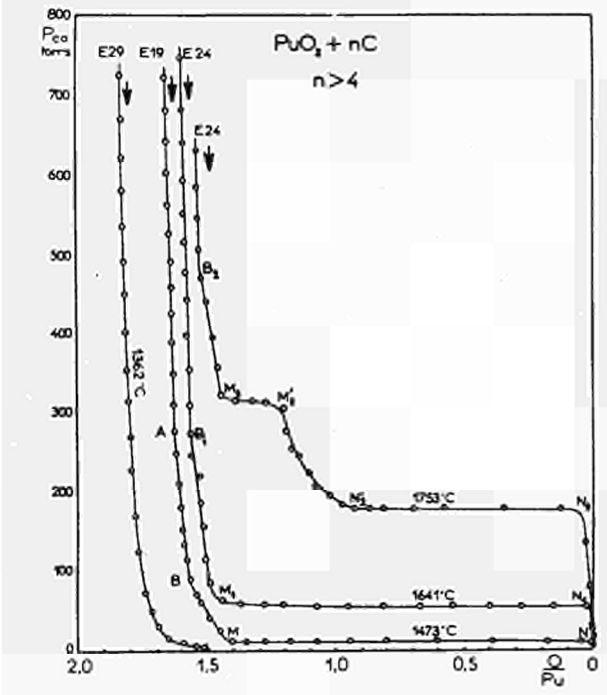

FIG. 7 The carbothermic reduction of PuO_2 (ref 17)

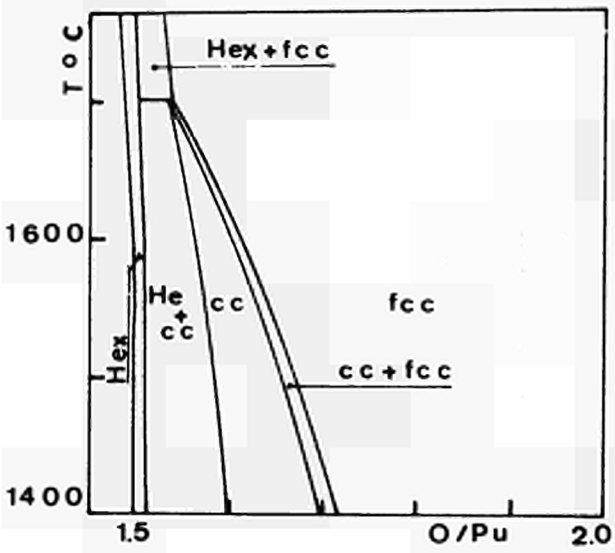

FIG. 8 A plutonium-oxygen phase diagram (ref 17)

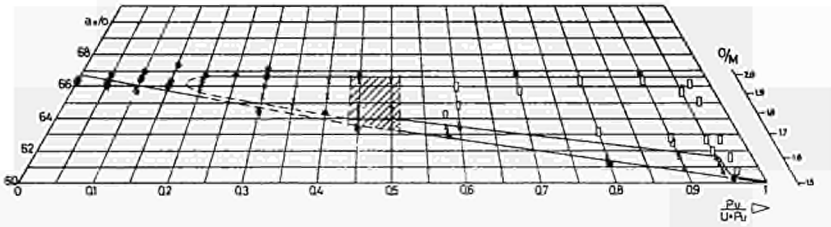

FIG. 9 Isothermal section at room temperature of the U-Pu-O diagram between O/M = 1.5 and O/M = 2.00 ○ single phase fcc; Δ single phase bcc; x two fcc phases; □ fcc+bcc; ⊗ fcc+metal; ▫ bcc+metal; ⊗ hex. Pu_2O_3 (ref 20)

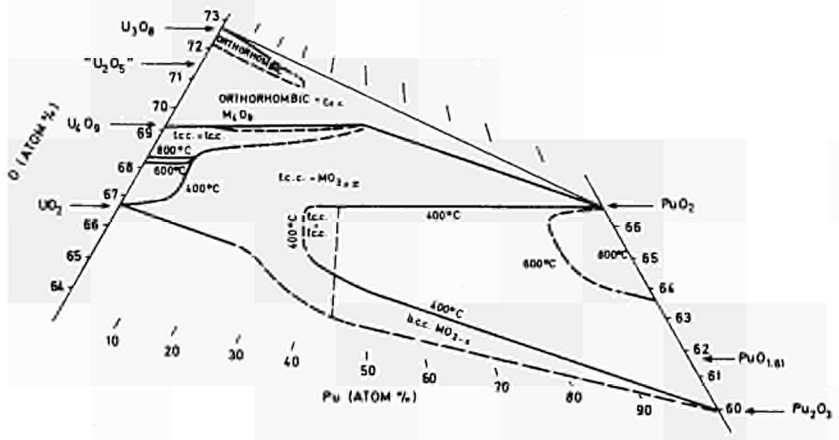

FIG. 10 A U-Pu-O ternary section at 400, 600 and 800°C (ref 13, 22)

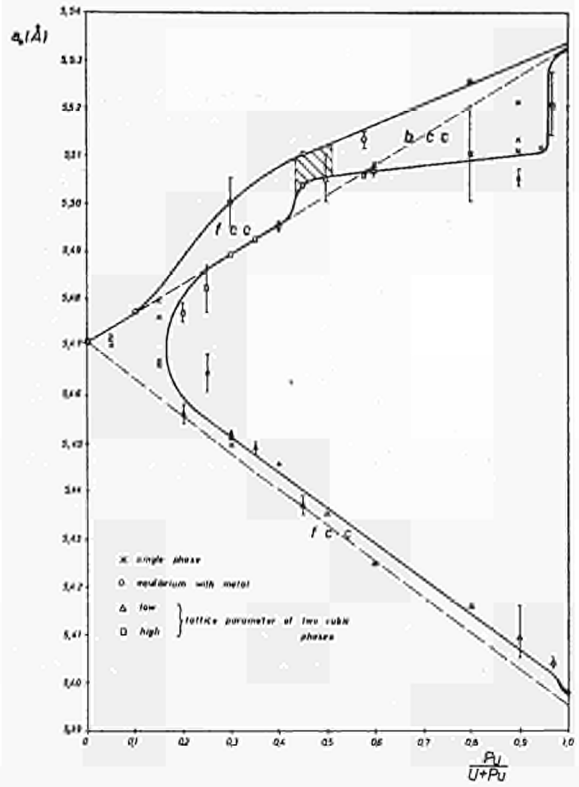

FIG. 11 Cubic lattice parameters plotted as a function of plutonium content. Bcc parameters are plotted at half their value ——— limit of cubic single phase region - - - - Vegard lines (ref 20)

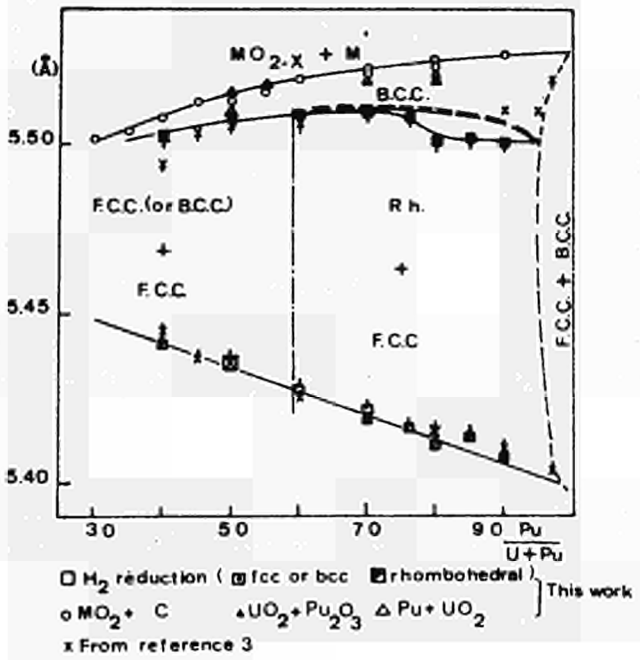

FIG. 12 Lattice parameters for the U-Pu-O system (ref 18)

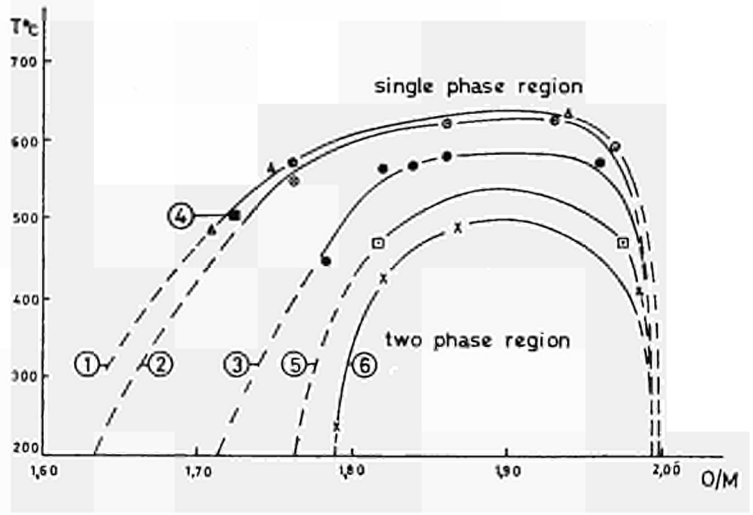

FIG. 13 Limits of the two-phase region determined by DTA. Pu/(U+Pu) ratios are (1) 1, (2) 0.95, (3) 0.8, (4) 0.58 (ref 22), (5) 0.58, (6) 0.42 (ref 22) (ref 20)

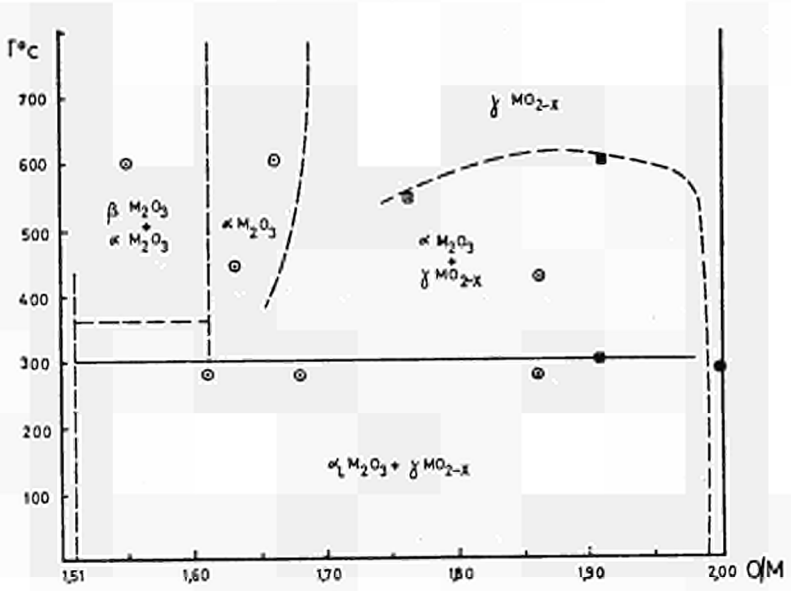

FIG. 14 Pseudo binary diagram M_2O_3-MO_2 at Pu/(U+Pu) = 0.97 (M=U+Pu). ⊙ X-ray diffraction and ceramography. ⊡ D.T.A. (ref 20)

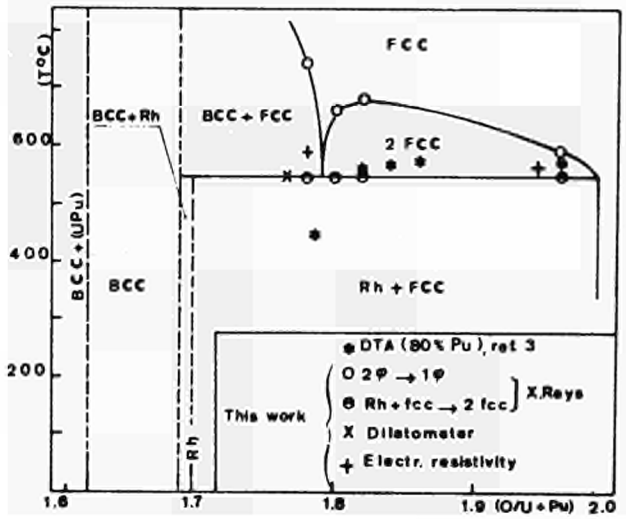

FIG. 15 Pseudo binary diagram U-Pu-O at $^{Pu}/U+Pu = 0.76$ (ref 18)

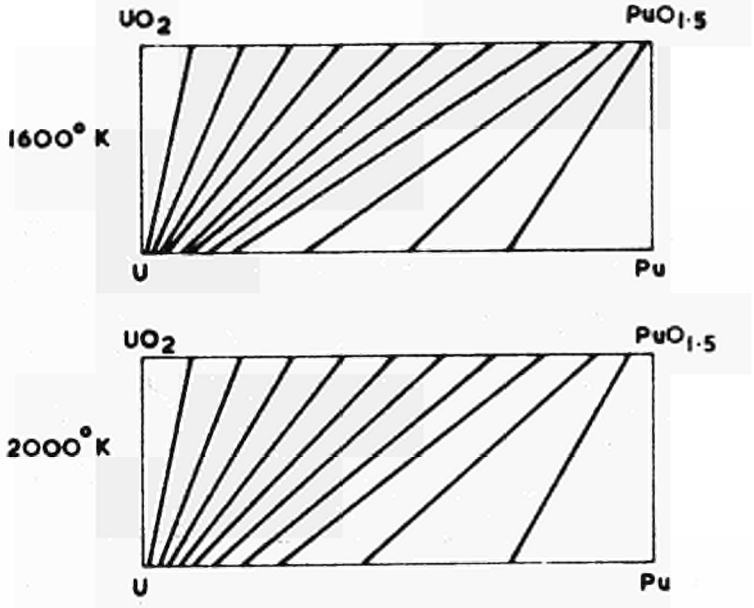

FIG. 16 Equilibria in the phase field $U_{1-x_1}Pu_{x_1}$ (liquid) + $U_{1-x_2}Pu_{x_2}O_{2-0.5x_2}$ Solid (ref 23)

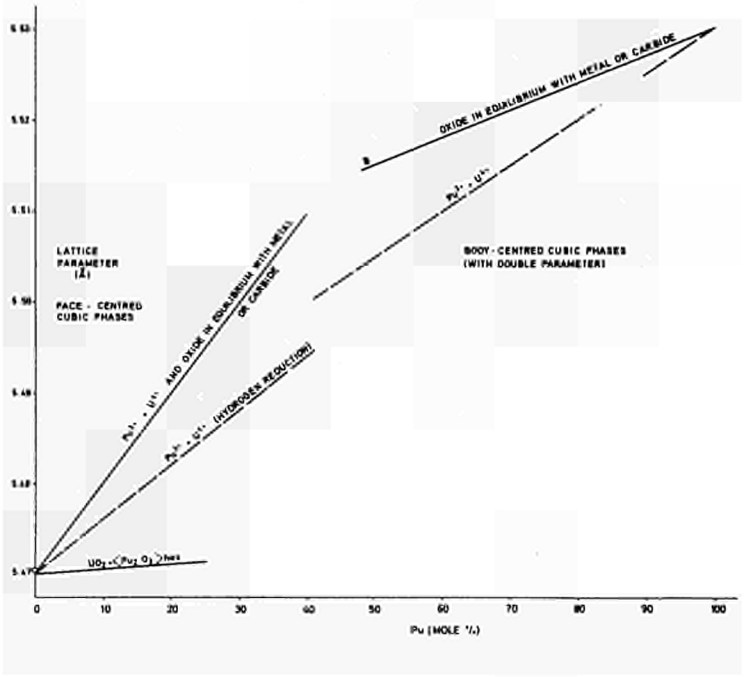

FIG. 17 Lattice parameters of "fully-reduced" uranium-plutonium oxides (ref 13)

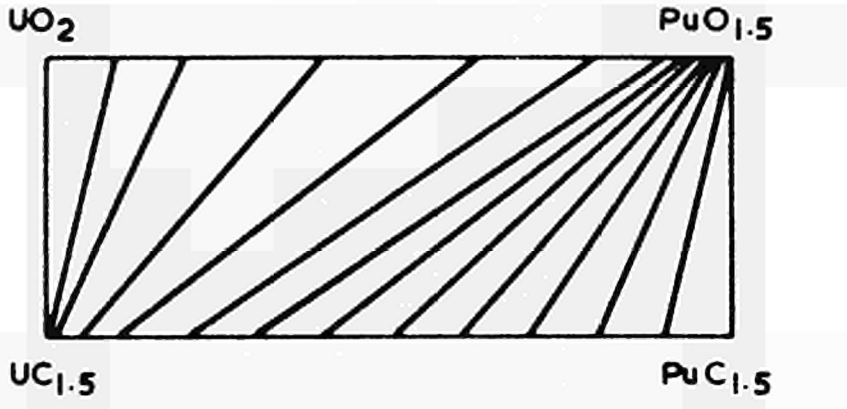

FIG. 18 Equilibria in the phase field $U_{1-x_2}Pu_{x_2}O_{2-0.5x_2}$(solid) + $U_{1-x_3}Pu_{x_3}C_{1.5}$(solid) (ref 23)

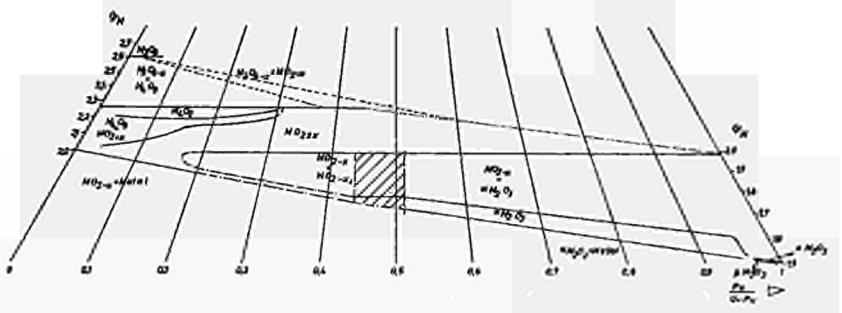

FIG. 19 Room temperature section for U-Pu-O (ref 20)

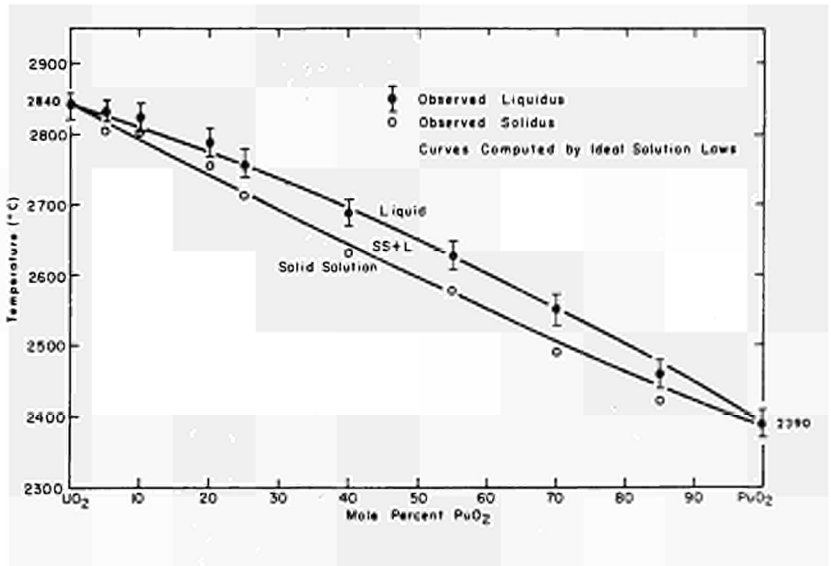

FIG. 20 Solid-liquid phase diagram for the UO_2-PuO_2 system (ref 24)

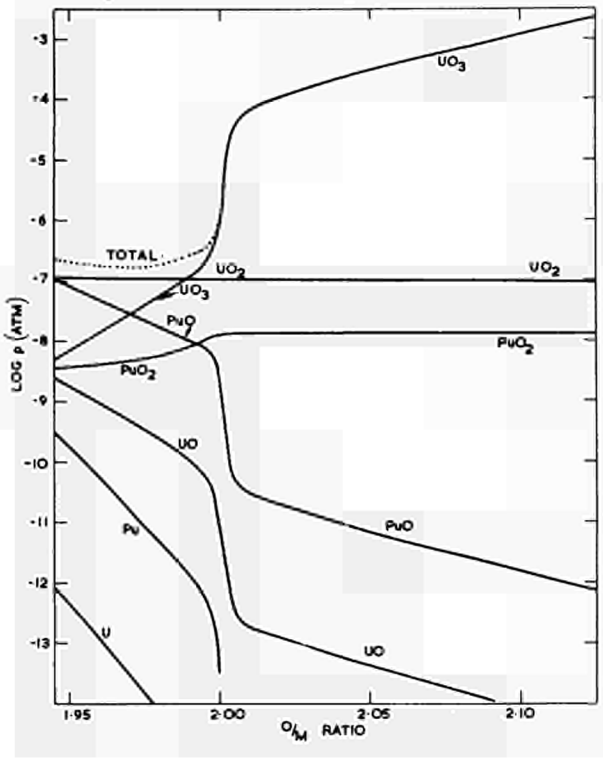

FIG. 21 Partial pressures over $U_{0.85}Pu_{0.15}O_{2\pm y}$ at 2000°K(calculated) (ref 27)

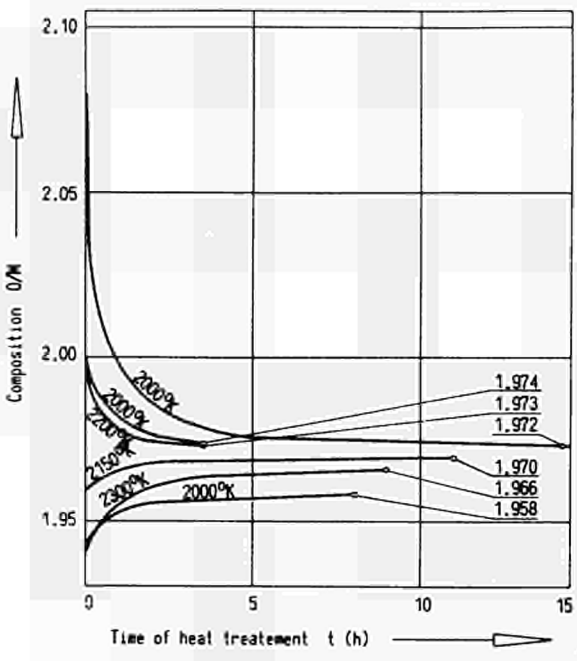

FIG. 22 Rate of change of composition O/M of $(U_{0.85}Pu_{0.15})O_{2\pm y}$ at constant temperature in UHV (ref 28)

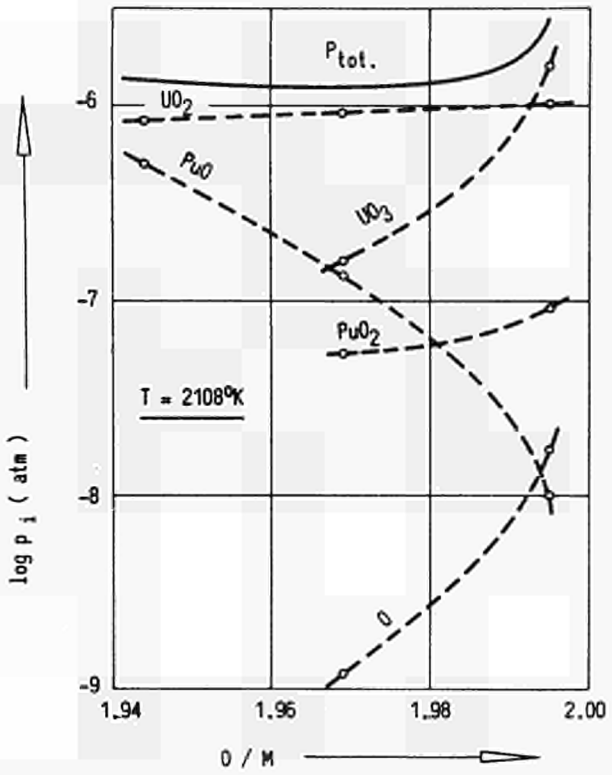

FIG. 23 Partial pressure - composition diagram of UO_3, UO_2, PuO_2, PuO and O over $(U_{0.85}Pu_{0.15})O_{2-y}$ at 2103°K (ref 28)

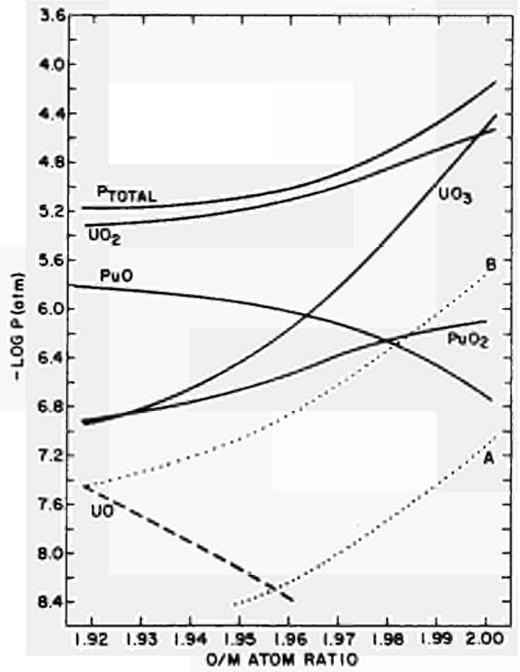

FIG. 24 Partial Pressures of the Vapor-Species over $(U_{0.8}Pu_{0.2})O_{2-x}$ at 2241°K (ref 29)

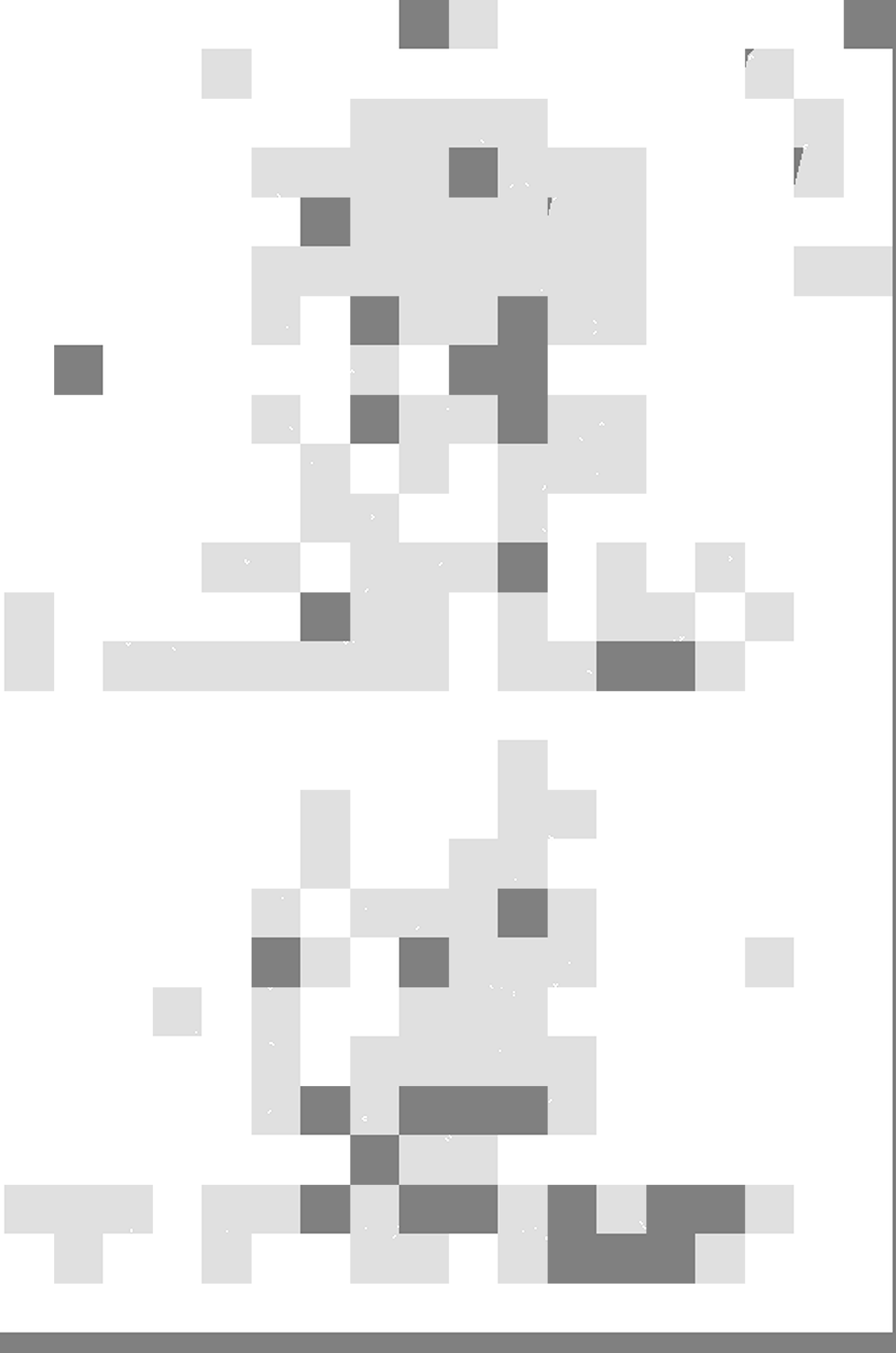

2. Fission product phase diagrams

Some aspects of the phase equilibria for the major fission products with uranium and plutonium oxides are discussed together with the application of the principles of phase equilibria in predicting the chemical state of a 'burnt' fuel.

Some attempt to predict the chemical state of burnt oxide fuels using thermochemical data were reported by Rand and Roberts (1). At burn-ups of ca. 10 % of all the U and Pu relatively large quantities of some of the fission product elements will be produced. The thermodynamical data for the oxides allows some predictions to be made concerning the chemical composition of this 'multicomponent' oxide system.

The approach to predict the final chemical composition is simply to use an Ellingham diagram (Fig. 1) for the oxides of the fission product elements, together with that for the fuel oxide, so that the oxygen partial molal free energy ($\Delta \bar{G}_{O_2}$) of the system is a minimum. However, a complication is whether the oxides formed are soluble in the fuel matrix or whether they are present as separate phases, and whether ternary phases can form. To answer these questions detailed observations on irradiated fuels must be made on extremely well characterized materials; but some progress can be made by simply having some knowledge of the phase relationships of the fission product elements with the U-O and Pu-O systems. The earlier calculations for thermal fission (1) of $U^{235}O_2$ were extended by Rand and Markin (2) for a fuel composition $U_{0.85}Pu_{0.15}O_2$ subjected to a fast neutron flux, and to a burn-up of 7 % of the heavy atoms.

The fission product elements can be divided into the following groups:

a) those such as Ba, Sr, Zr, Y, and the rare earth which form very stable oxides,

b) Nb, Mo, Tc with oxides whose oxygen potentials are quite close to that of the fuel together with those which form

very unstable oxides such as Rh, Ru, Pd,

c) Cs, Rb which will form a liquid phase at the operating temperature of the fuel elements, and will most likely condense in the colder regions of the fuel elements; I is also considered here, and

d) Te and Se.

The rare gases of course will not form compounds under these conditions.

Aspects of the phase equilibria are now discussed.

2.1. The group of fission products Ba, Sr, Y and the rare earths

2.1.1. The Ba-U-O system

McIver (3) heated mixtures of UO_2 and BaO together at 1500°C under a controlled oxygen potential of -110 Kcal.mole$^{-1}O_2$. For Ba concentrations up to a Ba/U+Ba ratio of 0.1, no variation in the lattice parameter of UO_2 was found and it was concluded that under these conditions of temperature and oxygen potential Ba does not dissolve in UO_2. Ba forms ternary compounds with U and O, $BaUO_3$ has a perovskite structure (cubic Pm3m), and there are a series of Ba uranates containing 6-valent U (4). The compounds are BaU_2O_7 (tetragonal), $Ba_2U_3O_{11}$, $BaUO_4$ (orthorhonbic), and Ba_3UO_6. These compounds with 6-valent U would only be expected to form in an environment with a very high oxygen potential (fuel O/M > 2.00).

2.1.2. The Ba-Pu-O system

Because of the slightly smaller ionic radius for a given valence for Pu compared with U, it is to be expected that Ba would be insoluble in PuO_2, and in the presence of Pu^{3+} the solubility may be higher. Again the perovskite $BaPuO_3$ compound exists with the $BaTiO_3$ structure (5). Ba plutonates with higher plutonium valencies exist at correspondingly higher oxygen potentials (6).

2.1.3. The Sr-U-O system

McIver (3) found the lattice parameter of UO_2 decreased in the

presence of SrO at 1500°C in the presence of oxygen at a potential of -110 Kcal.mole^{-1} O_2. The variation in parameter was given by a_o = 5.4700 - 0.0046 x Å where x is the mole% of SrO (maximum ca. 12 mole%).

There are again a series of uranates (with 6 valent U) SrU_4O_{13}, $Sr_2U_3O_{11}$, $SrUO_4$, Sr_2UO_5, Sr_3UO_6. $SrUO_6$ has an α-rhombohedral form isomorphous with $CaUO_4$, and a ß-orthorhombic form isomorphous with $BaUO_4$. Cordfunke and Loopstra (7) have measured the heat of solution of these compounds in nitric acid and have calculated the values for the heat of formation (ΔH^o_{f298}) as SrU_4O_3 - 1424Kcal-mole^{-1} (estimated), $Sr_2U_3O_{11}$ - 1242 Kcal.mole^{-1}, α-$SrUO_4$ - 469.6 Kcal.mole^{-1}, ß-$SrUO_4$ - 469.9 Kcal.mole^{-1}, Sr_2UO_5 - 617.2 Kcal. mole^{-1}, Sr_3UO_6 - 760.2 Kcal.mole^{-1}.

2.1.4. The Sr-Pu-O system

A cubic perovskite $SrPuO_3$ exists as well as compounds containing 6-valent Pu (5,6).

2.1.5. The Ba-Zr-O and Sr-Zr-O systems

Zr being a major fission product as well as Sr and Ba, the possibility of the formation of Ba and Sr zirconates in irradiated fuels must be considered, solid solutions of the form $Ba_{1-x}Sr_xZrO_3$ with a perovskite structure may be formed under certain conditions.

The formation of the Ba and Sr uranates, plutonates and zirconates or solid solutions of all components, namely $Ba_{1-x}Sr_x(U_{1-y-z}Pu_yZr_z)O_3$ and the equilibria with BaO and SrO and also with the mixed U,Pu oxides with some solubility of Zr in the oxide matrix are very complex problems but it would be interesting to obtain correlations between the oxygen potential of the fuel matrix and the chemical form of the grey inclusions containing Ba. In some calculations of the chemical state of an irradiated fuel (8) the formation of $BaZrO_3$ has been assumed, and there has been some evidence for this compound from studies by Bradbury et al (9) on irradiated UO_2. Ba and Zr were found together with some Sr by microprobe analysis.

Schmitz (10) simulated a $U_{0,8}Pu_{0.2}$ oxide fuel with 25 fission product elements with a burn-up of 2%; the O/M ratio was 1.978. A grey phase was found in the simulated oxide which was a (U-Pu) Ba-O phase. However, in a simulation experiment reported by Schmitz et al (11) in which 16% burn-up was simulated in a $U_{0.8}Pu_{0.2}$ oxide fuel, a grey phase containing Ba and Zr but with no U and Pu was found. Oi and Tanabe (12) found that Ba was segregated on the surface of slightly irradiated single crystals of UO_2. O'Boyle et al (13) examined a UO_2-20wt% PuO_2 with O/M = 2.00 irradiated in a fast neutron flux to a burn-up of 2.7%. Microprobe analysis revealed a grey phase which contained Ba, Sr and Ce. The Ce was believed to be a daughter product of ^{140}Ba that originated from the decay chain:

16 sec Xe → 66 sec Cs → 12.8 day ^{140}Ba → 40.2 h La → stable Ce.

^{140}Ba is probably stable for a sufficient time to nucleate before decaying to Ce.

Clearly the conditions under which these various phases containing Ba, Sr, Zr and sometimes U and Pu will require further assessment.

The eutectic temperature for BaO and $BaZrO_3$ and for SrO and $SrZrO_3$ are given as (14) 2000° and 2200° C at ca. 50 mole% BaO and ca. 20 mole% SrO.

2.1.6. The U-Zr-O-system

Cohen and Schaner (15) investigated the phase relationships in this system and presented data for temperatures greater than 1000°C. The phase diagram presented by these authors is shown in Fig. 2. A continuous solid solution was established in the temperature range 2300 to 2550°C. This solid solution has the fluorite structure. Pure ZrO_2 undergoes two transitions monoclinic - tetragonal (1170 ± 20°C) and tetragonal-cubic (2285 ± 15°C) before the melting point is reached (2710 ± 30°C). A two-phase region was found above 1660°C and extends to ca. 2300°C on the ZrO_2-rich composition side. The phases in this region are f.c.cubic and f.c.tetragonal. The tem-

perature at which the ZrO_2-rich phase in the two-phase region transforms to the monoclinic structure was given as $\sim 100^{\circ}C$, and the solubility of ZrO_2 in UO_2 was given as $\sim$ 12 mole%.

Romberger et al (16) extended these phase equilibria studies to lower temperatures by the use of a molten fluoride 'flux' which provided a means of readily obtaining the equilibrium phases at temperatures less than $1200^{\circ}C$. The revised phase diagram is shown in Fig. 3, and when compared with Fig. 2 it is seen that the later study indicates a more rapid decrease in the mutual solubility of the cubic and tetragonal phases below $1600^{\circ}C$. The eutectoid temperature is given as $1110^{\circ}C$, this is a much higher temperature than the previous estimate. The eutectoid composition was at 2.8 mole% UO_2.

2.1.7. The Pu-Zr-O system

The earlier work on this system (17) has been recently extended by Mardon et al (18). These studies on samples with O/M ratios 1.61 to 2.00 showed that the stabilization of cubic ZrO_2 by PuO_2 to room temperature as previously observed is related to the presence of reduced oxides, the compositions of which lie on the $PuO_{1.61}$-ZrO_{2-x} tie line. In the fully oxidised state tetragonal ZrO_2 is stabilised over a wide range of PuO_2 contents at high temperatures whilst at lower temperatures the solubility of PuO_2 in the tetragonal phase appears to pass through a maximum at ca. $1000^{\circ}C$ and then decreases rapidly, leaving a wide two-phase region of PuO_2-rich cubic $(Pu,Zr)O_2$ plus ZrO_2-rich tetragonal $(Pu,Zr)O_2$.

In PuO_2-rich samples there is evidence of the existence of fluorite, C-type rare-earth oxide and pyrochlore structures at different oxygen potentials. The pyrochlore structure is based on the composition $Pu_2Zr_2O_7$. A possible room temperature isothermal section for PuO_2-$PuO_{1.5}$-ZrO_2 is shown in Fig. 4

The lattice parameters for the fluorite PuO_2-ZrO_2 solution do not deviate from Vegard's law.

A comparison of the U-Zr-O and Pu-Zr-O phase relationship

The phase relationships show a number of regions of similarity but also marked differences.

Both systems have complete solubility in the cubic phase field at high temperatures, extensive solubility in tetragonal ZrO_2 and only limited solubility in monoclinic ZrO_2. In the case of the Pu system, stabilisation of tetragonal ZrO_2 occurs over a much wider composition and temperature than in the U-system and there does not appear to be any eutectoidal decomposition of the tetragonal phase into cubic plus monoclinic structures as observed in the UO_2-ZrO_2 system.

The solubility limit of ZrO_2 in the fluorite cell of PuO_2 is significantly higher at low temperatures than is the solubility of ZrO_2 in UO_2 (14); this may reflect the slightly more favourable size difference between the PuO_2 and ZrO_2 cells than between UO_2 and ZrO_2 cells, 5% and 7% respectively.

Romberger et al (15), however, obtained very low figures for the mutual solubilities of UO_2 and ZrO_2 at temperatures below 1200°C. For the low and high temperature data to be consistent large deviations from ideality for the solid solutions must occur.

The Zr formed in fission will be dissolved in the fluorite solid solution of the fuel matrix, this has, indeed, been found in the examination of irradiated oxides (13) as well as Y and the rare earths. There is an extensive region of fluorite solid solution at the actinide-rich end of these systems.

2.1.8. The U-Y-O system

Bartram et al (19) have described the phase relationships in the region UO_3-UO_2-Y_2O_3 of this ternary system. A phase diagram for the temperature range 1000°-1700°C is shown in Fig. 5. In the diagram the solid lines represent established phase boundaries and the long-dash lines represent probable boundaries which are not well established. The short-dash lines denote the approximate composition line for three experimental conditions (a) hydrogen - 40°C dew point, 1700°C; (b) air 1000°C, and (c) 10 CO_2/CO

at 1500°C. The phase diagram shows a U_3O_8 phase, a f.c.c. fluorite cubic solid solution phase, a b.c.c. phase (rare earth C-type oxide) and two rhombohedral phases. The rhombohedral phases occur over a range of yttria compositions but at a constant oxygen to metal ratio of 1.71 and 1.87. The solubility of Y_2O_3 in the f.c.c. fluorite solid solution ranges from 0 to 50 mole% Y_2O_3 in dry hydrogen at 1700°C, and from 33 to 60 mole% Y_2O_3 in air at 1000°C. As the yttria concentration is increased above 18 mole% the fluorite-U_3O_8 phase boundary follows close to the MO_2 composition line. The b.c.c. solid solution extends from 80 to 100 mole% Y_2O_3 in hydrogen; however, in air above 1000°C there is little or no solubility of UO_3. Low temperature oxidation gives a maximum ratio for O/M of ca. 1.56 for the b.c.c. solid solution.

2.1.9. The U-La-O system

Diehl and Keller (20) have recently published data on the UO_2-UO_3-$LaO_{1.5}$ system. A section of the phase diagram at 1250°C is shown in Fig. 6. At 1250°C the following features were observed:

a) No La solubility in ß-U_3O_8.

b) The fluorite $(U,La)O_{2\pm x}$ exists over a considerable range of composition.

c) A rhombohedral phase 1, an ordered phase which occurs at the limiting compositions UO_3 $6LaO_{1.5}(M_7O_{12})$ with U^{6+}, and UO_2 $6LaO_{1.5}(M_7O_{11})$ with U^{4+}, and with a phase width corresponding to the compositions $UO_{2.5}5LaO_{1.5}$ and $UO_{2.5}$ $7LaO_{1.5}$.

d) A rhombohedral phase II, this phase extends from 71.5 to 76,5 mole% $LaO_{1.5}$ for U(VI) and shows only little phase width with respect to O/M ratio. Above 1310°C this ordered phase transforms reversibly to a disordered phase having a fluorite structure.

2.1.10. The U-Nd-O system

The system UO_2-UO_3-$NdO_{1.5}$ has recently been described by Boroujerdi (21). At 1250°C this system was found to consist of four single-phase regions and three two-phase regions, a section of the system is shown in Fig. 7. The single-phase regions are, ß-U_3O_8

and no solubility of $NdO_{1.5}$ could be detected; the f.c.c. fluorite phase $(U,Nd)O_{2\pm x}$ which covers a large area of the system. The limiting metal:oxygen compositions in this phase are $MO_{1.60}$ and $MO_{2.25}$. A rhombohedral phase occurs with limiting compositions $UO_2\ 6NdO_{1.5}$ and $UO_3\ 6NdO_{1.5}$. No variation in the U and Nd concentrations was found; this is a different behavior to the La system. There is no solubility of U in the hexagonal A-type $NdO_{1.5}$ lattice.

In the quasi-binary section UO_{2+x}-$NdO_{1.5}$($p(O_2)$ = 1 atm) the phase width of the fluorite phase $(U,Nd)O_{2\pm x}$ increases with rising temperature.

2.1.11. The U-Ce-O system

Using high temperature X-ray powder techniques Markin et al (22) constructed a ternary phase diagram between UO_2-U_3O_8 and CeO_2-$CeO_{1.81}$ for all concentrations of Ce and for temperatures between room-temperature and 600°C. Reduction of oxides to a hypostoichiometric composition where $z > 0.35$ for $U_{1-z}Ce_zO_{2+x}$ results in the formation of two phases $MO_{2.00}$ and MO_{2-x} in equilibrium at room temperature. Upon heating the two-phase product a single-phase is formed at a temperature dependent on the value of z. The O/M ratios of the MO_{2-x} phase correspond only to a partial reduction of Ce^{IV} to Ce^{III} and represent an intermediate phase. In this respect the Ce-O (23) and the U-Ce-O systems are similar. Reduction of oxides with $z < 0.35$ results in a single f.c.c. phase at all temperatures. Partial oxidation to a hyperstoichiometric composition when $z < 0.5$ results in either a single-phase f.c.c. MO_{2+x}, or MO_{2+x} in equilibrium with an M_4O_9 phase. Further oxidation causes the disappearance of the MO_{2+x} phase; the M_4O_9 phase is then in equilibrium with a M_3O_{8-y} type phase.

Partial oxidation to a hyperstoichiometric composition when $z > 0.5$ results in a single-f.c.c. MO_{2+x} phase. Phase diagrams at room temperature, 200°, 400°, 600°C are shown in Fig. 8. UO_2 and CeO_2 solid solutions obey Vegard's law.

Markin and Crouch (24) used a gas equilibrium technique to obtain thermodynamic data at 800 - 950°C, that is oxygen potentials for

hypostoichiometric U-Ce-O ($U_{1-x}Ce_xO_{2-y}$) where $0.10 < z < 0.75$. Plots of partial molal enthalpy and entropy for the system show great similarity to plots for the (U,Pu) oxides but a very different behaviour to the pure oxide system, CeO_{2-x} and PuO_{2-x}. The similarity between enthalpy plots for the mixed oxides supports the idea that O vacancies cannot locally order in the presence of moderately high concentrations of U(IV) ions.

The relationships between Ce valency and $\Delta\bar{G}_{O_2}$ are shown in Fig. 9, and do not lie on one plot for all concentrations as for the $(U,Pu)O_{2\pm x}$ system.

2.1.12. The U-Gd-O system

Some studies on this system have been described by Beale at al (25). Solid solutions between UO_2 and Gd_2O_3 prepared by sintering the oxides together at 1700°C in dry hydrogen exist up to Gd/U+Gd ratios of 0.80; the solutions had a f.c.c. structure and the relation between lattice parameter and Gd concentration was linear. The O/U+Gd ratios were not determined.

2.1.13. The Pu-Ce-O system

The only work reported on the rare earth-Pu-O systems, that is for the rare earths which are present in reasonable quantities, is on the Pu-Ce-O. Mulford and Ellinger (27) have shown that the lattice parameters for solid solutions of CeO_2-PuO_2 obey Vegard's law.

2.2. The fission product elements: Nb, Mo, Tc, Ru, Rh, and Pd

The oxides of the first three elements, namely Nb, Mo, and Tc form oxides which are more stable than Ru, Rh, and Pd. Nb is considered to be present in an oxidized state as a separate phase.

The transition metals Mo, Tc, Ru, Rh, and Pd are present in the form of a single-phase alloy which has been identified in irradiated oxide fuels (9,13,28-32). The actual concentration

of the elements in these inclusions depends on the temperature and position in the irradiated fuel.

Bramman et al (30) extracted these inclusions from the burnt oxide fuel of initial composition. $U_{0.85}Pu_{0.15}O_2$ which had been irradiated in the Dounreay Fast Reactor to 8-8.5% burn-up. The composition of the mechanically extracted inclusions was Mo 39.1 wt%, Tc 14.2 Wt%, Ru 30.4 wt%, Rh 6.7 wt%, and this alloy had an hexagonal structure with $a_o = 2.73 \pm 0.02$ Å, $c_o = 4.444 \pm 0.04$ Å. An attempt was made to prepare a synthetic alloy containing the same quantities of Mo, Tc, Ru and Rh by Bramman et al, but some Rh was lost during the preparation, the composition was (normalised to 100% total) Mo 43.5 wt%, Te 17.7 wt%, Ru 35.5 wt%, Rh 3.3.wt%. Although the X-ray diffraction pattern indicated the presence of only a single-phase hexagonal structure with cell size $a_o = 2.761 \pm 0.002$Å, $c_o = 4.439 \pm 0.005$ Å, examination by micro-probe analysis showed signs of a second-phase (5% volume) which had a composition close to Mo_5RuTc. The melting point of the alloy was between 1800 and 1900°C. The hexagonal alloy has the same structure as the Mo-Ru alloys with the hexagonal close packed phase - ε-phase (33). This structure extends from 45 to 82 at % Rh, and the lattice parameters accurate to $\pm$ 0.0002 Å were:

At % Rh	Annealing Temperature °C	a_o Å	c_o Å
45.2	1700	2.7597	4.4347
58.7	1750	2.7435	4.3907
80.9	1760	2.7199	4.3464

The chemically extracted inclusions in the studies of Bramman et al (30) were found to have some Pd present. A composition was given as Mo 41.0 wt%, Tc 14.9 wt%, Ru 31.9 wt%, Rh 7.1 wt%, Pd 2.0 wt%. One of the reasons why the composition of the alloy inclusion changes with radial position is that the alloy can oxidise to form MoO_2 providing the O_2 potential is high enough.

This phenomenon is illustrated in the studies of Davies and Ewart (34), when the inclusions in two irradiated plutonium oxides of different initial stoichiometry were examined. The composition of the inclusions is given below.

Initial fuel composition	Composition range of inclusions in irradiated plutonium oxides				
	Mo	Tc	Ru	Rh	Pd
$PuO_{1.7}$	8.5-1.5 (11.7)	4.2-8.4 (6.1)	7.8-15.7 (12.1)	4.6-6.9 (5.8)	6-10.8 (9.5)
$PuO_{2.0}$	0.3-1.5 (0.9)	1.2-3.1 (1.7)	5.9-15.3 (8.0)	1.3-6.6 (3.7)	0.9-13.2 (7.9)

(average values in brackets)

Although there are very large scatters on the results it is apparent that for the oxide with the higher stoichiometry not only Mo but also Tc has been oxidised.

TcO_2 is less stable than MoO_2 by more than 20 Kcal.mole^{-1}. Thus, when the alloys are oxidised it would be expected that MoO_2 will be formed and not until all the Mo has been oxidised will Tc be oxidised. It is also worthwhile noting that the reaction

$$\langle Mo \rangle + (O_2) \rightleftharpoons \langle MoO_2 \rangle$$

may not buffer the oxygen potential in a burnt fuel. The Mo is not at unit activity, dissolved in the 5-component alloy (Mo-Tc-Ru-Rh-Pd) and immediately the alloy is oxidising the Mo concentration and thus its activity decreases and higher oxygen potentials are required to oxidise the alloy. If ideal solution is assumed for Mo in the alloy, its atom fraction will be ca. 0.30. The oxygen potentials required to oxidise pure Mo and Mo of lower activities, i.e. for the reaction

$$[Mo] + (O_2) \rightleftharpoons \langle MoO_2 \rangle .$$

A difference of ca. 14 Kcals. at 2000 K is found for the oxygen potential for the above reaction when $a_{Mo} = 1$, and $a_{Mo} = 0.03$. This is illustrated in Fig. 10.

O'Boyle et al also extracted an inclusion from irradiated oxide materials (13) with the composition 20.0 wt% Mo, 16.6 wt% Tc, 48.6 wt% Ru, 12.9 wt% Rh, 2.0 wt% Pd. U, Pu, C,N,O were not detected and there was a tendency for both Mo and Pd to migrate towards the colder regions of the fuel. An alloy was prepared with the same composition as the inclusion and was found to have an hexagonal structure with $a_o = 2.735 \pm 0.001$ and $c_o = 4.355 \pm 0.001$ Å.

In the irradiated oxides examined by Bramman et al (30) a second cubic metallic phase adjacent to the Mo-Tc-Ru-Rh-Pd-alloy was found. The composition of this inclusion was 25.4 wt% U, 13.5 wt% Pu, 38.4 wt% Pd, 11.9 wt% Rh, and 2.5 wt%Ru. The lattice parameter of this cubic phase was $a_o = 4.127 \pm 0.002$ Å. Clearly, this compound is of the Cu_3Au type, and similar to URu_3 (35) and URh_3 which have lattice parameters $a_o = 3.988$ Å and $a_o = 4.063$ Å, respectively.

It has to be expected that the U and Pu concentrations in this alloy would be different from the fuel matrix, namely Pu/U+Pu = 0.15.

Schmitz et al (11) also observed this phase in a simulation of oxide fuel at 16 % burn-up. Microprobe analysis showed there to be a UPd_3 phase present in addition to the expected Mo-Tc-Ru-Rh-Pd alloy, in this simulation this alloy contained Re as a substitute for Tc, and also some Nb.

The formation of these actinide-group VIII element alloys is curious at the stated initial oxygen, concentrations of the fuel were close to 2 in the studies of Bramman et al and in those of Schmitz et al. The free energy of formation of URu_3 has been measured by Holleck and Kleykamp (36) using a CaF_2 electrolyte galvanic cell in the temperature range 1000-1140°K. The value for the free energy of formation was $\Delta G^o_{f\,\langle URu_3\rangle} = -53800 + 8.4\,T$ cal. $mole^{-1}$. Campbell et al (37) measured the free energy of formation

of $PuRu_2$ (there is no $PuRu_3$ compound in the Pu-Ru system) using an E.M.F. cell with a liquid chloride electrolyte in the temperature range 935-1069°K, which was given as

$$\Delta G^{o}_{f\,\langle PuRu_2\rangle} = -26800 + 6{,}9\ T \text{ cal.mole}^{-1}$$

The compounds of the U systems are most likely more stable than the corresponding alloys of the Pu system. Where the U potentials of the region Ru + URu_3 are extrapolated to the temperatures appropriate to a fuel element, the equilibrium U oxide would be hypostoichiometric UO_{2-x}. This is borne out by the observations that actinide-group VIII element compounds can only be made by reaction of the oxide and metal in very reducing atmospheres (i.e. dry hydrogen)(38).

2.3. The systems involving Cs, Rb, and I

Cs and Rb have very low melting points, 30° and 39°C, respectively, and because of their high vapour pressures are expected to be found in the colder regions of the fuel element, namely, in the region between the fuel and the cladding.

Some iodine will also be found in this liquid phase; this liquid phase will also dissolve oxygen; the amount of oxygen depending on the oxygen potential of the fuel surface. A relation is required between the oxygen potential and oxygen concentration for these Cs-Rb-O-I solutions.

The mode of reaction between this solution and the stainless steel cladding materials will depend markedly on the oxygen potential; the conditions under which compounds in the ternary systems Cs-Cr-O, Cs-Mo-O form are not yet known. The formation of Cs (and Rb) uranates and plutonates must also be considered as is also required for a 'failed' fuel element pin situation where sodium primary coolant can come into direct contact with the oxides, and then the formation of sodium uranates and plutonates and the conditions under which they form must be considered (39).

Ohse and Schlechter (40) have considered several aspects of the role of Caesium in fuel-cladding interactions.

2.4. The Te and Se systems

Te has been found associated with Ag in the region of the metallic-transition element inclusions by Huber and Kleykamp (31) in irradiated $U_{0.15}Pu_{0.85}O_{1.98} \pm 0.01$.

The actual chemical form of both these fission products is not known although due to their high vapour pressures they could migrate via the gas phase to the colder regions of the fuel elements.

U and Pu oxy-tellurides and oxyselenides are known to exist but the actual oxygen potential at which these compounds form has not been determined. There are, of course, a series of U and Pu tellurides and selenides.

2.4.1. The U-Te-O system

The ternary compound UOTe has been reported (41) to possess a tetragonal symmetry of the PbFCl type with lattice parameters a_o = 4.004 Å, c = 7.491 Å. A second ternary phase U_2O_2Te has recently been identified (42) with a b.c.tetragonal cell(a_o = 3.964 C_o=12.346 Å) and as isomorphous with the rare earth oxytellurides (43). A tentative phase diagram for this system at 1200°C has been given by Breeze (44) and is shown in Fig. 11. The oxygen potential for the phase fields in which the oxytellurides are present would be required before any assessment as to their likely presence in a "burnt' oxide fuel can be made.

2.4.2. The Pu-Te-O system

Pu_2O_2Te is the only reported ternary compound of the system as is reported to be isomorphous with U_2O_2Te (45).

2.4.3. The U-Se-O system

Breeze (44) has also presented a possible phase diagram for this system at 600°C, see Fig. 12. Again the oxygen potentials of the phase fields involving UOSe the only ternary compound of the system are required. UOSe crystallises with a tetragonal sym-

metry with a PbFCl type phase with lattice parameters a_o=3.9005 Å and c_o = 6.9823 Å. No evidence was obtained by Breeze for a U_2O_2Se compound.

2.4.4. The Pu-Se-O system

No data is available for the ternary phase diagram but two ternary compounds exist, PuOSe with a tetragonal (P4/mmm) structure (a_o = 4.151 Å c_o = 8.369 Å), and Pu_2O_2Se which is not isomorphous with U_2O_2Te but crystallises with the A-type hexagonal La_2O_3 structure (a_o = 3.957 Å c_o = 6.977 Å) (46).

References:

1. M.H. RAND, L.E.J. ROBERTS, Thermodynamics Vol.I, I.A.E.A. Vienna 1966, p.3
2. M.H. RAND, T.L. MARKIN, Thermodynamics of Nuclear Materials 1967, I.A.E.A. Vienna 1968,p.637
3. E.J. McIVER, UKAEA report AERE M-1612 (1966)
4. G.G. ALLPRESS, J.Inorg.Nucl.Chem. 26 (1964) 1847
5. L.E. RUSSELL, J.D.L. HARRISON, N.H. BRETT, J.Nucl.Mat. 2 (1960) 310
6. C. KELLER, Nucleonik 4 (1963) 271
7. C. CORDFUNKE, B.O. LOOPSTRA, J.Inorg.Nucl.Chem. 29 (1967) 51
8. F. ANSELIN, USAEC report BEAP-5583 (1969)
9. B.T. BRADBURY, J.T. DEMANT, P.M. MARTIN, UKAEA report AERE-R 5149 (1966)
10. F.SCHMITZ, Ceramic Nucl.Fuels. Proceedings of the international symposium. Nuclear Div. Amer.Ceram.Soc., Spec.Pub.2 (Eds.O.L. Kruger, A.I. Kaznoff) Columbus,Ohio 1969, p. 32
11. F. SCHMITZ, G. DEAN, M. ROUSSEAU, F. de KEROULAS, J.C.van CRAEYNEST, Proceedings of international meeting on fast reactor fuel elements (ed. M. Dalle Donne, K. Kummerer, K. Schroeter), GfK Karlsruhe 1970, p.396
12. N.OI, I.TANABE, J.Nucl.Mat. 29 (1968) 288
13. D.R. O'BOYLE, F.L. BROWN, J.E. SENECKI, J.Nucl.Mat. 29 (1969) 27
14. H.v. WASTENBERG, W.GURR, Z.anorg. u.allgem.Chem. 196 (1931)381
15. I.COHEN, B.E.SCHANER, J.Nucl.Mat. 9 (1963) 18
16. K.ROMBERGER, C.F. BAESjr., H.H. STONE, J.Inorg.Nucl.Chem. 29 (1967) 1619
17. D.F. CARROLL, USAEC report HW-69305 (1961)
18. P.G.MARDON, D.J.HODKIN, J.T. DALTON, J.Nucl.Mat.32 (1969)126
19. S.F. BARTRAM, E.F.JUENKE, E.A. AITKEN, J.Amer.Ceram.Soc. 47 (1964) 171
20. H.G.DIEHL, C.KELLER, J.Solid State Chem. 3 (1971) 621
21. A.BOROUJERDI, GfK report KFK 1330 (1971)
22. T.L. MARKIN, R.S. STREET, E.C. CROUCH, J.Inorg.Nucl.Chem.32 (1970) 59

23. D.J. BEVAN, J. KORDIS, J.Inorg.Nucl.Chem.26 (1964) 1509
24. T.L. MARKIN, E.C. CROUCH, J.Inorg.Nucl.Chem. 32 (1970) 77
25. T.L. MARKIN, E.J.McIVER, Plutonium 1965 (eds. A.E.Kay, M.B. Waldron), London Chapman and Hall 1967, p.845
26. R.J. BEALE, J.H. HANDWERK, B.J. WRONA, J.Amer.Ceram.Soc. 52 (1969) 578
27. R.N.R. MULFORD, F.H. ELLINGER, J.Phys.Chem. 62 (1958) 1466
28. B.T. BRADBURY, J.T. DEMANT, P.M. MARTIN, D.M. POOLE, J.Nucl. Mat. 17 (1965) 227
29. B.M. JEFFERY, J.Nucl.Mat. 22 (1967) 33
30. J.L. BRAMMAN, R.M. SHARPE, D. THOM, G. YATES, J.Nucl.Mat. 25 (1968) 201
31. H. HUBER, H. KLEYKAMP, GfK report KFK 1324 (1972)
32. D.R. O'BOYLE, F.L. BROWN, A.E. DWIGHT, J.Nucl.Mat. 35 (1970)257
33. E.ANDERSON, W.HUME-ROTHERY, J.Less-Common Metals 2 (1960) 19
34. J.H. DAVIES, F.T. EWART, J.Nucl.Mat. 41 (1971) 143
35. J.I. PARK, J.Res.Natl.Buro Standards 72A (1968) 1
36. H. HOLLECK, H. KLEYKAMP, J.Nucl.Mat. 35 (1970) 158
37. G.M. CAMPBELL, L.J. MULLINS, J.A. LEARY, Thermodynamics of Nucl.Mat. 1967, I.A.E.A. Vienna 1968, p.75
38. B.ERDMANN, C. KELLER, J.Inorg.Nucl.Chem. 7 (1971) 675
39. E.H.P. CORDFUNKE, B.O. LOOPSTRA, J.Inorg.Nucl.Chem. 22 (1971) 2427
40. R.W. OHSE, M.SCHLECHTER, paper to this Panel
41. A.J. KLEIN-HANEVELD, F.JELLINEK, J.Inorg.Nucl.Chem. 26 (1964) 1127
42. E.W. BREEZE, N.H. BRETT, J.Nucl.Mat. 40 (1971) 113
43. R. BALLESTRACCI, Compt.Rend. 264 (1967) 1736
44. E.W. BREEZE, Ph.D.thesis, Department of Ceramics, University Sheffield 1971
45. M. ALLBUTT, A.R. JUNKISON, U.K.A.E.A. report AERE-R 5541 (1967)
46. C. KELLER, The Chemistry of the Transuranium Elements, Verlag Chemie 1971, p. 398

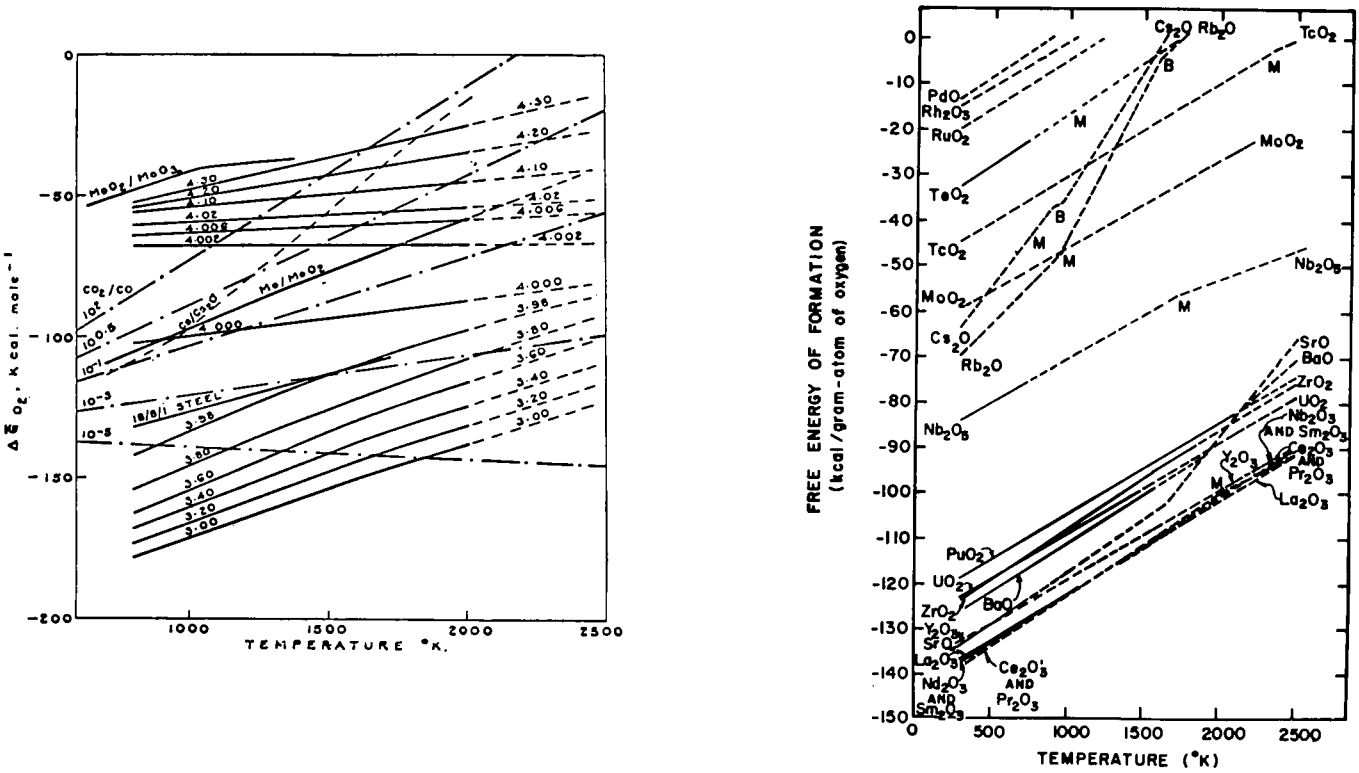

FIG. 1a and 1b Ellingham Diagrams of oxygen potentials of systems of relevance to burnt oxide fuels.

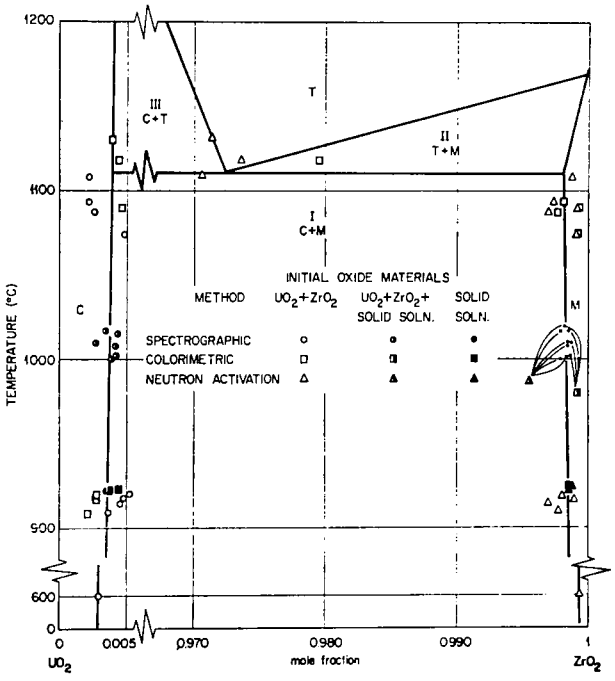

FIG. 2 The UO_2-ZrO_2 temperature-composition diagram from 600 to 1200°C. The phase designations are: C, face-centered cubic; T, face-centered tetragoncl; M, monoclinic. (ref 16)

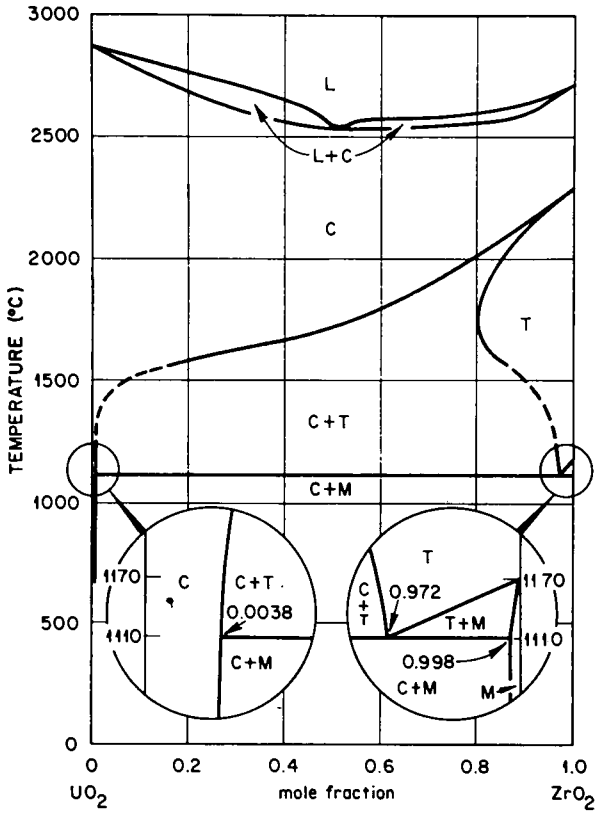

FIG. 3 Revised UO_2-ZrO_2 phase equilibrium diagram. The phase designations are: L, liquid; C, face-centered cubic; t, face-centered tetragonal; M, monoclinic. (ref 16)

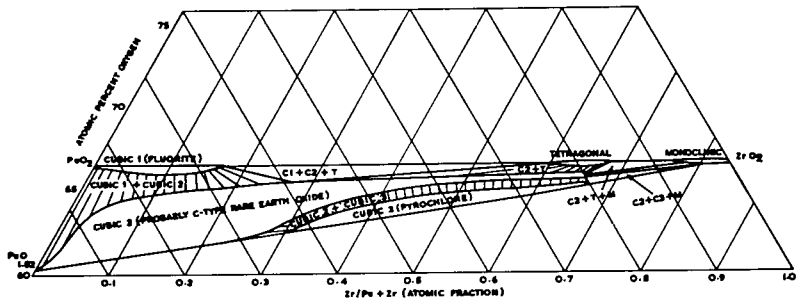

FIG. 4 Proposed room-temperature isothermal section PuO_2-$PuO_{1.5}$-ZrO_2 (ref 18)

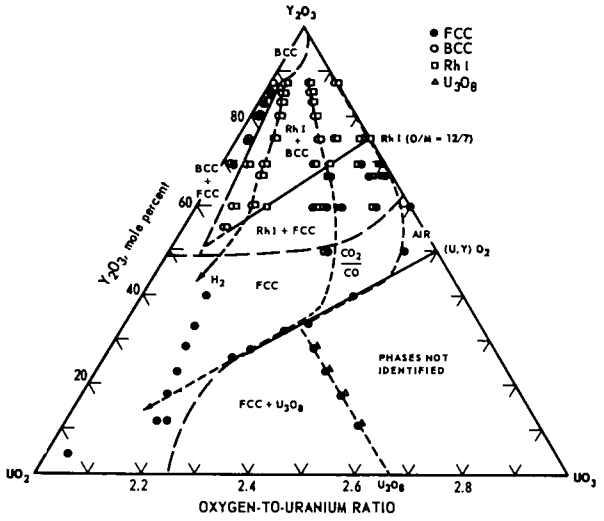

FIG. 5 The UO_2-UO_3-Y_2O_3 ternary diagram from 1000° to 1700°C (ref 19)

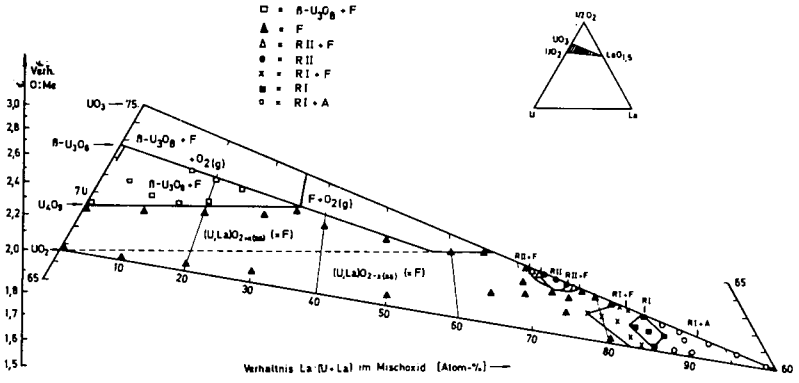

FIG. 6 A section of the phase diagram for the ternary system U-La-O at 1250°C (ref 20)

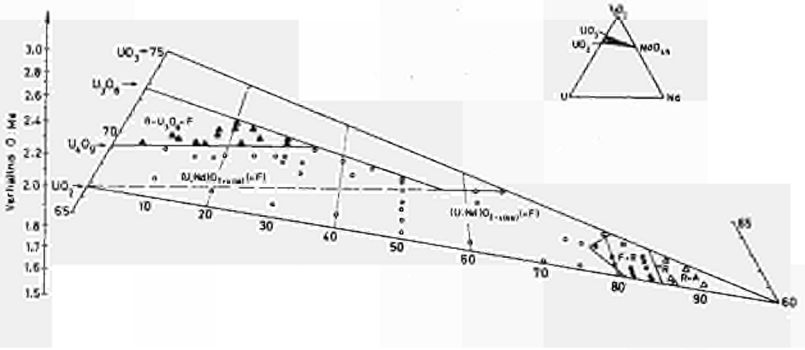

FIG. 7 A section of the phase diagram for the ternary system U-Nd-O at 1250°C (ref 21)

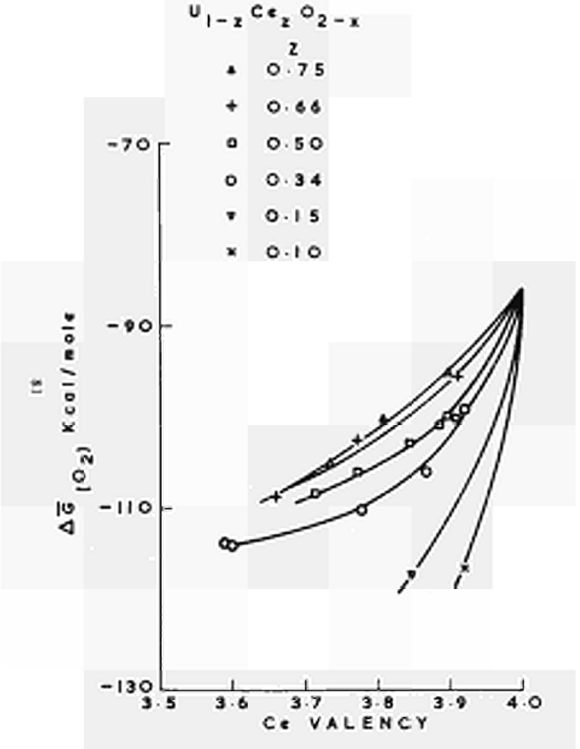

FIG. 9 $\Delta\bar{G}_{(O_3)}$ VS. Ce valency at 800°C (Ref 24)

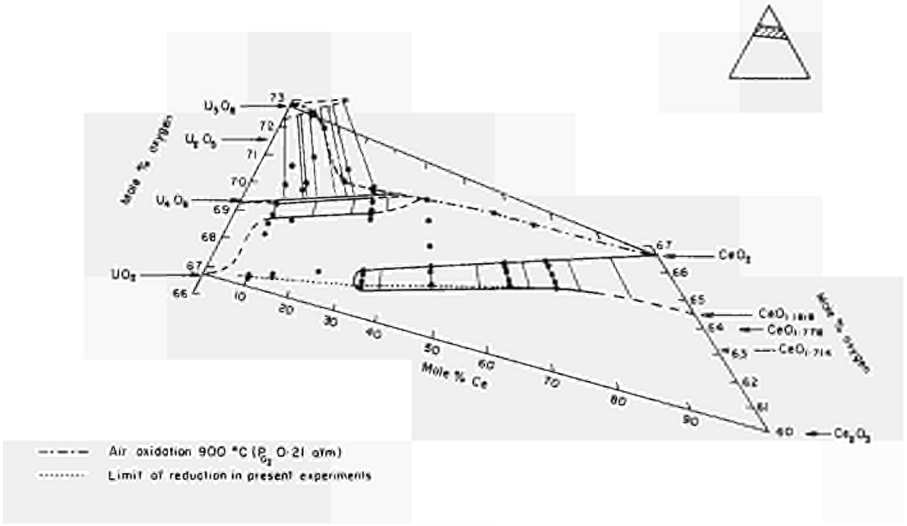

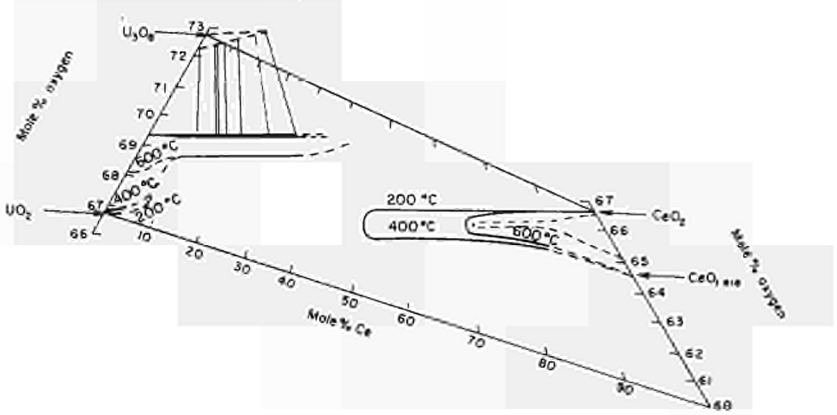

FIG. 8 U-Ce-O ternary phase diagram at (a) room temperature (b) 200, 400 and 600°C

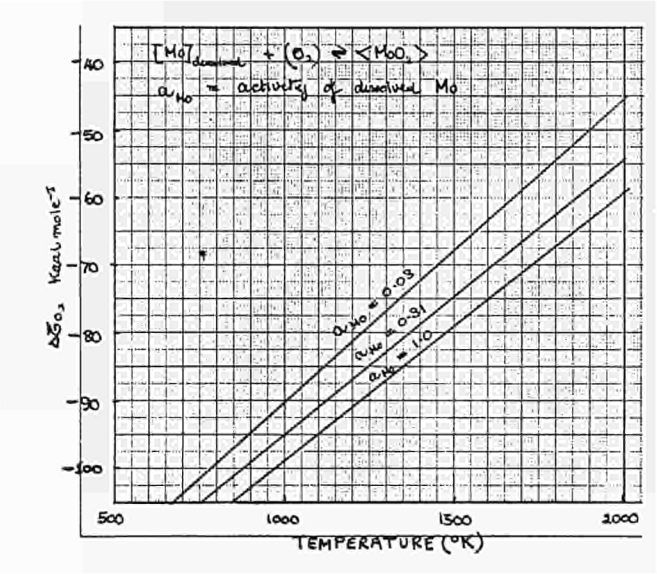

FIG. 10 The effect of change of Mo activity on the oxygen potentials for the reaction $Mo + O_2 = MoO_2$

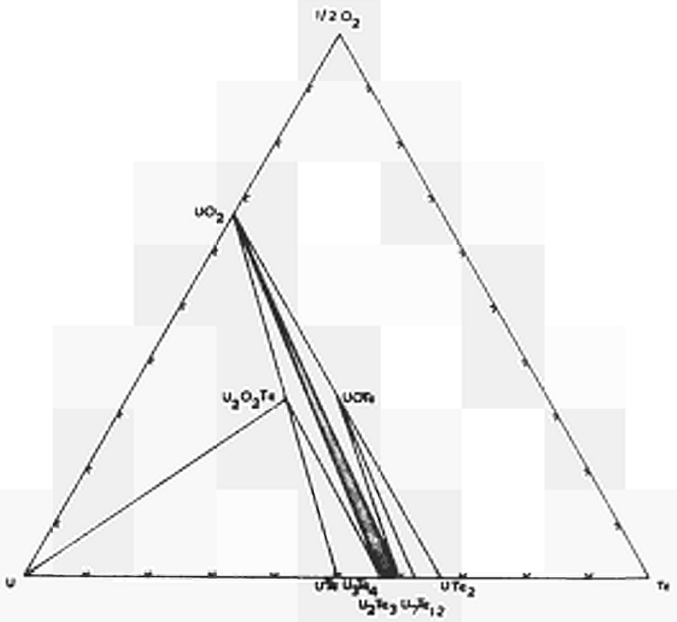

FIG. 11 A section of the U-Te-O system at 1200°C (ref 44)

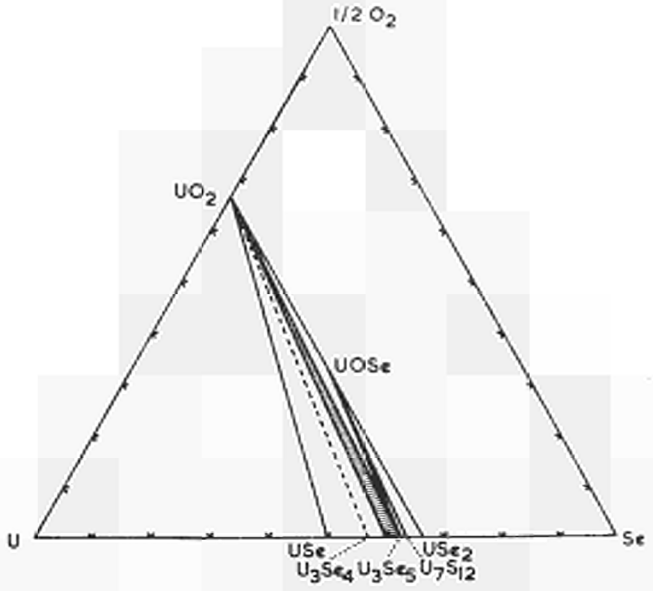

FIG. 12 A section of the U-Se-O system at 600°C (ref 44)

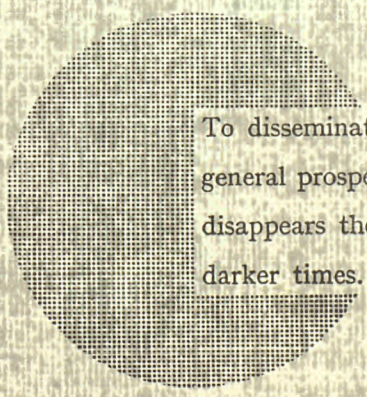

To disseminate knowledge is to disseminate prosperity — I mean general prosperity and not individual riches — and with prosperity disappears the greater part of the evil which is our heritage from darker times.

Alfred Nobel

SALES OFFICES

The Office for Official Publications sells all documents published by the Commission of the European Communities at the addresses listed below, at the price given on cover. When ordering, specify clearly the exact reference and the title of the document.

UNITED KINGDOM

H.M. Stationery Office
P.O. Box 569
London S.E. 1 — Tel. 01-928 69 77, ext. 365

BELGIUM

Moniteur belge — Belgisch Staatsblad
Rue de Louvain 40-42 — Leuvenseweg 40-42
1000 Bruxelles — 1000 Brussel — Tel. 12 00 26
CCP 50-80 — Postgiro 50-80

Agency :
Librairie européenne — Europese Boekhandel
Rue de la Loi 244 — Wetstraat 244
1040 Bruxelles — 1040 Brussel

DENMARK

J.H. Schultz — Boghandel
Møntergade 19
DK 1116 København K — Tel. 14 11 95

FRANCE

Service de vente en France des publications des Communautés européennes — Journal officiel
26, rue Desaix — 75 732 Paris - Cédex 15e
Tel. (1) 306 51 00 — CCP Paris 23-96

GERMANY (FR)

Verlag Bundesanzeiger
5 Köln 1 — Postfach 108 006
Tel. (0221) 21 03 48
Telex: Anzeiger Bonn 08 882 595
Postscheckkonto 834 00 Köln

GRAND DUCHY OF LUXEMBOURG

Office for Official Publications of the European Communities
Case postale 1003 — Luxembourg
Tel. 4 79 41 — CCP 191-90
Compte courant bancaire: BIL 8-109/6003/200

IRELAND

Stationery Office — The Controller
Beggar's Bush
Dublin 4 — Tel. 6 54 01

ITALY

Libreria dello Stato
Piazza G. Verdi 10
00198 Roma — Tel. (6) 85 08
CCP 1/2640

NETHERLANDS

Staatsdrukkerij- en uitgeverijbedrijf
Christoffel Plantijnstraat
's-Gravenhage — Tel. (070) 81 45 11
Postgiro 42 53 00

UNITED STATES OF AMERICA

European Community Information Service
2100 M Street, N.W.
Suite 707
Washington, D.C., 20 037 — Tel. 296 51 31

SWITZERLAND

Librairie Payot
6, rue Grenus
1211 Genève — Tel. 31 89 50
CCP 12-236 Genève

SWEDEN

Librairie C.E. Fritze
2, Fredsgatan
Stockholm 16
Post Giro 193, Bank Giro 73/4015

SPAIN

Libreria Mundi-Prensa
Castello 37
Madrid 1 — Tel. 275 51 31

OTHER COUNTRIES

Office for Official Publications of the European Communities
Case postale 1003 — Luxembourg
Tel. 4 79 41 — CCP 191-90
Compte courant bancaire: BIL 8-109/6003/200

OFFICE FOR OFFICIAL PUBLICATIONS OF THE EUROPEAN COMMUNITIES
Case postale 1003 — Luxembourg 6147